DMD Fast Forward. Published on April 23, 2015 as DOI: 10.1124/dmd.115.064170
This article has not been copyedited and formatted. The final version may differ from this version.

SLCO1A2-MDCKII: a Promising in vitro System to Understand the Role of OATP1A2 in Blood Brain Barrier Drug Penetration

Houfu Liu, Na Yu, Sijie Lu, Sumito Ito, Xuan Zhang, Bhagwat Prasad, Enuo He, Xinyan Lu, Yang Li, Fei Wang, Han Xu, Gang An, Jashvant D. Unadkat, Hiroyuki Kusuhara, Yuichi Sugiyama and Jasminder Sahi

Drug Metabolism and Pharmacokinetics (H.L., N.Y., S.L., X.L., Y.L., F.W., J.S.) and Molecular Discovery Research (H.X., G.A.), Platform Technology and Science, GlaxoSmithKline R&D Shanghai, China; Modelling and Translational Biology (E.H.), Platform Technology and Science, GlaxoSmithKline, Ware, UK; Department of Molecular Pharmacokinetics, Graduate School of Pharmaceutical Sciences, University Of Tokyo, 7-3-1 *Hongo, Bunkyo-ku, Tokyo* 113-0033*, Japan (S.I., X.Z., H.K.); Sugiyama Laboratory, RIKEN Innovation Center, Research Cluster for Innovation, RIKEN, 1-6 Suehiro-cho, Tsurumi-ku, Yokohama-shi, Kanagawa 230-0045, Japan (Y. S.), and Department of Pharmaceutics, University of Washington, Seattle, Washington 98195-7610, United States (B.P., J.D.U.)*

Downloaded from dmd.aspetjournals.org at ASPET Journals on April 19, 2024

DMD Fast Forward. Published on April 23, 2015 as DOI: 10.1124/dmd.115.064170
This article has not been copyedited and formatted. The final version may differ from this version.

Running title: A NOVEL SLCO1A2-MDCKII SYSTEM TO UNDERSTAND UPTAKE ACROSS BBB

Corresponding author: Jasminder Sahi, GlaxoSmithKline R&D Shanghai, 898 Halei Road, Zhangjiang Hi-Tech Park, Shanghai 201203, China.

Office phone number: (+86-21) 6159 0637. Fax number: (+86-21) 6159 0730. E-mail: jasminder.j.sahi@gsk.com

Number of Text Pages: 34

Number of Tables: 1

Number of Figures: 10

Number of References: 48

Number of Words in Abstract Section: 244

Number of Words in Introduction Section: 731

Number of Words in Discussion Section: 1153

ABBREVIATIONS: BBB, blood-brain barrier; BCRP, breast cancer resistance protein; CNS, central nervous system; $E_2$17βG, 17β-estradiol-17β-D-glucuronide; HEK, human embryonic kidney; KO; knock-out; LC, liquid chromatography; MDCK, Madin-Darby canine kidney; MOI, multiplicity of infection; MS, mass spectrometry; OATP, organic anion-transporting polypeptide; P-gp, P-glycoprotein; RT-PCR, reverse transcriptase polymerase chain reaction; SLCO, solute carrier family of the OATPs; TCA, taurocholic acid; WT, wild type.

Downloaded from dmd.aspetjournals.org at ASPET Journals on April 19, 2024

DMD Fast Forward. Published on April 23, 2015 as DOI: 10.1124/dmd.115.064170
This article has not been copyedited and formatted. The final version may differ from this version.

Abstract

OATP1A2 has the potential to be a target for CNS drug delivery due to its luminal localization at the human blood-brain barrier and broad substrate specificity. We found OATP1A2 mRNA expression in human brain to be comparable to BCRP and OATP2B1 and much higher than P-gp and confirmed greater expression in brain relative to other tissues. The goal of this study was to establish a model system to explore OATP1A2-mediated transcellular transport of substrate drugs and the interplay with P-gp. In vitro (HEK293 cells stably expressing Oatp1a4, the closest murine isoform) and in vivo (naïve and Oatp1a4 knock-out mice) studies with OATP1A2 substrate triptan drugs demonstrated that these drugs were not Oatp1a4 substrates. This species difference demonstrates that the rodent is not a good model to investigate active brain uptake of potential OATP1A2 substrates. Thus, we constructed a novel OATP1A2 expressing MDCKII-wild type (WT) and MDCKII-MDR1 system using BacMam virus transduction. The spatial expression pattern of OATP1A2 after transduction in MDCKII-MDR1 cells was superimposed to P-gp, confirming apical membrane localization. OATP1A2-mediated uptake of zolmitriptan, rosuvastatin and fexofenadine across monolayers increased with increasing OATP1A2 protein expression. OATP1A2 counteracted P-gp efflux for co-substrates zolmitriptan and fexofenadine. A three-compartment model incorporating OATP1A2-mediated influx was used to quantitatively describe the time- and concentration-dependent apical-to-basolateral transcellular transport of rosuvastatin across OATP1A2 expressing MDCKII monolayer. This novel, simple and versatile experimental system is useful for understanding the contribution of OATP1A2-mediated transcellular transport across barriers such as the blood brain barrier.

Downloaded from dmd.aspetjournals.org at ASPET Journals on April 19, 2024

DMD Fast Forward. Published on April 23, 2015 as DOI: 10.1124/dmd.115.064170
This article has not been copyedited and formatted. The final version may differ from this version.

Introduction

The blood-brain barrier (BBB) presents a major hurdle to the delivery of drugs to the central nervous system (CNS). The capillary endothelium of the BBB is among the most restrictive barriers with tight junctions that preclude paracellular distribution, as well as efflux transporters that effectively limit transcellular passage of more permeable xenobiotics. To enable brain uptake of essential polar nutrients, highly specialized uptake systems are expressed at the BBB for example for glucose and amino acids. While the role of efflux transporters in protecting the brain from exposure to potential toxins is well appreciated, the involvement of BBB uptake transporters in brain penetration of drugs is poorly understood. Human OATP1A2 (rodent Oatp1a4) has emerged as a potentially important BBB uptake transporter for drugs (Urquhart and Kim, 2009). An indication of the potential of OATP1A2 as a brain drug delivery target comes from studies with statins that are OATP substrates and demonstrate neuroprotection in hypoxia and inflammatory disorders, including multiple sclerosis (Ciurleo et al., 2014; Sierra et al., 2011). OATP1A2 (SLCO1A2) is a member of the sodium-independent uptake transporter family that was initially reported exclusively expressed at human brain microvessels and not detected in astrocytes or neurons (Gao et al., 2000; Lee et al., 2005). It was later confirmed to be expressed on luminal membrane of BBB in tumorous and healthy adjacent tissue (Bronger et al., 2005), although a more recent paper reports expression in neurons as well (Gao et al., 2014). OATP1A2 transports amphipathic substrates, including bile salts, thyroid hormones, steroid conjugates, organic dyes and anionic oligopeptides, as well as xenobiotics (Franke et al., 2009). The substrate spectrum of OATP1A2 includes neuroactive substrates (i.e., opioid analgesic peptides), drugs with CNS side effects (e.g. the antibacterial levofloxacin that may cause seizures, toxic psychoses, increased intracranial pressure and CNS stimulation), and/or toxicities (e.g.

Downloaded from dmd.aspetjournals.org at ASPET Journals on April 19, 2024

DMD Fast Forward. Published on April 23, 2015 as DOI: 10.1124/dmd.115.064170
This article has not been copyedited and formatted. The final version may differ from this version.

methotrexate may cause mild white-matter changes or severe CNS demyelination and encephalopathy) (Badagnani et al., 2006; Gao et al., 2000; Maeda et al., 2007). There is no rodent orthologue reported for OATP1A2. Oatp1a4 and Oatp1c1 are two major isoforms expressed and enriched at mouse BBB (Cheng et al., 2005; Mayerl et al., 2012). The closest counterpart to OATP1A2 is Oatp1a4 (Slco1a4), which shares 72% gene homology. Unlike OATP1A2, Oapt1a4 is expressed at both the apical and basolateral membranes of the microvascular endothelium of the BBB (Gao et al., 1999; Ose et al., 2010). Oatp1a4 has a wide substrate spectrum that includes amphipathic organic anions such as 17β-estradiol-17β-D-glucuronide ($E_2$17βG) and statins (Kikuchi et al., 2004), prostaglandin E1 (Taogoshi et al., 2005) and morphine-6-glucuronide (Bourasset et al., 2003). Oatp1a4 functional expression at the rat BBB increases with pain and correlates with taurocholate transport across the BBB (Ronaldson et al., 2011). An earlier study from our laboratory showed that marketed triptans were substrates for OATP1A2 using BacMam2-OATP1A2 transduced HEK293 system, likely contributing to their ability to traverse the BBB (Cheng et al., 2012). We later confirmed naratriptan to be an OATP1A2 substrate as well (K_m 13.7 μM), using the same OATP1A2 expressing HEK293 system (data not published). Understanding the difference in expression of these two transporters at the BBB could improve predictions of CNS permeability of drug candidates.

Discovery-stage studies to assess CNS uptake potential are typically conducted in vitro using MDCK cells transfected with human P-gp, and in vivo in rodents to quantify brain distribution, as species difference in terms of P-gp substrate specificity and expression are minimal (Feng et al., 2008; Uchida et al., 2011b). Using in vitro human P-gp and rodent in vivo data for evaluating the CNS penetration potential of discovery compounds with >1% brain free fraction, we found cases where compounds with low P-gp efflux activity were not taken up into rodent brain, while

Downloaded from dmd.aspetjournals.org at ASPET Journals on April 19, 2024

DMD Fast Forward. Published on April 23, 2015 as DOI: 10.1124/dmd.115.064170
This article has not been copyedited and formatted. The final version may differ from this version.

some P-gp and/or BCRP substrates were detected at appreciable concentrations. While the former could be due to additional efflux transporters (e.g. MRP4, MRP5), the latter is most likely due to the presence of BBB uptake transporter(s) or low fraction of P-gp and/or BCRP contribution relative to passive permeability in preventing the CNS entry of the compounds (Hsiao and Unadkat, 2014). In this study, we have focused on OATP1A2 to evaluate the potential for this uptake transporter as a target for enhancing transcellular permeability in vitro. We have established novel methodologies using the BacMam virus and quantitatively characterized the role OATP1A2 transporter plays in uptake of its substrates in both wild-type and P-gp transfected cells.

Downloaded from dmd.aspetjournals.org at ASPET Journals on April 19, 2024

DMD Fast Forward. Published on April 23, 2015 as DOI: 10.1124/dmd.115.064170
This article has not been copyedited and formatted. The final version may differ from this version.

Materials and Methods

Materials

Zolmitriptan, almotriptan, sumatriptan, rizatriptan and naratriptan were purchased from Toronto Research Chemicals (Toronto, Canada); Rosuvastatin calcium salt from Santa Cruz Biotechnology (Santa Cruz, CA); Fexofenadine hydrochloride and Atenolol from Sigma (St. Louis, MO) and naringin was purchased from TCI (Tokyo, Japan). [^{3}H]Taurocholate acid (TCA) and [^{3}H]estradiol 17β-D-glucuronide ($E_2$17βG) were purchased from PerkinElmer (Boston, MA). Cell culture reagents were purchased from Invitrogen (Carlsbad, CA). All other reagents used were of bioanalytical grade or higher. For OATP1A2 quantification, peptide (EGLETNADIIK) standard was purchased from New England Peptides (Boston, MA). The corresponding stable isotope labeled ([$^{13}C_6$$^{15}N_2$]-lysine) internal standard was obtained from Thermo Fisher Scientific (Rockford, IL). The ProteoExtract native membrane protein extraction kit was procured from Calbiochem (Temecula, CA). The protein quantification bicinchoninic acid assay (BCA) kit, dithiotrietol, iodoacetamide and MS grade trypsin were purchased from Pierce Biotechnology (Rockford, IL).

Determination of the Brain-to-Plasma Concentration Ratios of Sumatriptan, Naratriptan and Zolmitriptan after Intravenous Infusion in Wild-Type and Oatp1a4 (−/−) Mice

Animal experiments in this study were performed according to the guidelines provided by the Institutional Animal Care Committee (Graduate School of Pharmaceutical Sciences, The University of Tokyo). Oatp1a4 (−/−) mice were obtained from Deltagen (San Carlos, CA) and their generation was described previously (Ose, et al., 2010). Wild-type (WT) C57BL/6J mice were supplied by Oriental Yeast Co., LTD (Tokyo, Japan). All mice were maintained under

Downloaded from dmd.aspetjournals.org at ASPET Journals on April 19, 2024

DMD Fast Forward. Published on April 23, 2015 as DOI: 10.1124/dmd.115.064170
This article has not been copyedited and formatted. The final version may differ from this version.

standard conditions with a 12-h reverse dark/light cycle. Food and water were available ad libitum.

Male C57BL/6J mice and Oatp1a4 (−/−) mice (10-18 weeks) weighing approximately 25-35 g were used for the experiments. Under pentobarbital anesthesia (30 mg/kg), the jugular vein was cannulated with polyethylene-10 catheter for the administration of drugs. The mice then received a constant intravenous infusion of sumatriptan, naratriptan, or zolmitriptan at a rate of 0.335, 0.288 and 0.313 μmol/h/kg, respectively. These compounds were dissoved in saline. Blood samples were collected from jugular vein at 30 and 60 min after treatment and brain and liver were excised immediately after blood collection at 60 min. Plasma specimens were obtained by centrifugation of the blood samples (10,000*g*). The plasma, brain, and liver concentrations of sumatriptan, naratriptan, and zolmitriptan were determined using LC-MS/MS analysis.

Determination of Cellular Uptake of Triptans Using a Stable Transfectant of mOatp1a4 in HEK293 Cells

Construction of the stable transfectant of Oatp1a4 in HEK293 cells was as described previously (Ose et al., 2010). Uptake was initiated by addition of the triptans to the incubation buffer after cells had been washed twice and preincubated at 37^{o}C for 10 min in Krebs-Henseleit buffer. Uptake was terminated at a specified time by addition of buffer at 4^{o}C, and cells were washed three times. The amount of triptans associated with the cells and medium was determined by LC-MS/MS analysis. The protein concentrations in aliquots of cell lysate were determined using Lowry's method. Triptan uptake was assessed from the cell-to-medium ligand concentration ratio, calculated as the concentration of triptans associated with the cells divided by that in the medium.

Construction of OATP1A2 Expressing MDCKII-WT or MDCKII-MDR1 Cells

Downloaded from dmd.aspetjournals.org at ASPET Journals on April 19, 2024

DMD Fast Forward. Published on April 23, 2015 as DOI: 10.1124/dmd.115.064170
This article has not been copyedited and formatted. The final version may differ from this version.

Generation of recombinant BacMam2-OATP1A2 baculovirus (second generation of BacMam vector) was described previously (Cheng et al., 2012). Polarized Madin-Darby canine kidney (MDCKII-WT or MDCKII-MDR1) cells were used for the in vitro transport studies and were obtained from The Netherlands Cancer Institute (Amsterdam, The Netherlands). Cell cultures and transport studies were conducted according to the procedure described previously (Rautio et al., 2006). BacMam2-OATP1A2 at an appropriate multiplicity of infection (MOI) was administered to the apical side of 24-well Transwell inserts (Millipore, Bedford, MA) 24 h post MDCKII cell seeding. The Transwell insert had a surface area of 0.33 cm^2 as specified by manufacturer. The cells were cultured for another 48 h before transport experiments.

Transport Studies across BacMam2-OATP1A2 Transduced or Non-transduced MDCKII-WT or MDCKII-MDR1 Cells

On the day of transport experiments, donor solutions were prepared by diluting test compounds in transport medium (Dulbecco's Modified Eagle Medium supplemented with 4500 mg/L D-glucose, L-glutamine, 25 mM HEPES but without sodium pyruvate and phenol red, pH 7.4). Receiver solution was the transport medium. The transport of test compounds was measured in both directions [apical to basolateral (A→B) and basolateral to apical (B→A)]. Lucifer yellow was used as a paracellular marker to determine the integrity of MDCKII monolayer and its concentration was measured using a SpectraMax Gemini cytofluorimeter (Molecular Devices, CA) set to an excitation wavelength of 430 nm and an emission wavelength of 540 nm. The permeability at pH 7.4 (P_{exact}) for test compounds across MDCKII monolayer was determined by the method described previously (Tran et al., 2004).

Membrane Localization of OATP1A2 in BacMam2-OATP1A2 Transduced MDCKII-MDR1 Monolayers by Immunocytochemical Staining

Downloaded from dmd.aspetjournals.org at ASPET Journals on April 19, 2024

DMD Fast Forward. Published on April 23, 2015 as DOI: 10.1124/dmd.115.064170
This article has not been copyedited and formatted. The final version may differ from this version.

The BacMam2-OATP1A2 transduced (MOI = 50) MDCKII-MDR1 monolayers were fixed in 4% paraformaldehyde on Transwell filter membranes for 15 min at room temperature. The fixed monolayers were subsequently incubated in 0.2% Triton X-100 for 2 min at room temperature, washed three times with PBS, and incubated with 10% normal goat serum in PBS to block non-specific antibody binding. The monolayers were washed three times with PBS and incubated overnight at 4^{o}C in a 1:200 dilution of rabbit anti-OATP1A2 antiserum (Santa Cruz Biotechnology, Inc, Santa Cruz, CA, USA) and a 1:50 dilution of mouse anti-MDR1 antibody (Sigma, St. Louis, MO). After incubation, the monolayers were washed three times with PBS and then incubated for 1 h at room temperature in a 1:1000 dilution of secondary antibodies (Alexa Fluor 546-conjugated anti-rabbit IgG and Alexa Fluor 488-conjugated anti-mouse IgG, Invitrogen). Subsequently, the monolayers were stained with diamidinophenylindole (DAPI, Sigma–Aldrich) for 2 minutes at room temperature. Finally, the MDCKII monolayers were transferred and mounted on glass slides and imaged by Nikon A1R inverted confocal microscope with 60X oil immersed lens (Plan Apo VC N.A. 1.40, Nikon). Images were captured and analyzed by NIS Element AR software. Fluorescence intensity along lines from apical to basal side were normalized by averaged intensity and plotted by Microsoft Excel software.

Quantification of Test Compounds by LC-MS/MS

Quantification of zolmitriptan, rosuvastatin, and fexofenadine in MDCKII transport samples was performed by Waters ACQUITY UPLC™ system coupled with Waters Xevo™ TQ mass spectrometry system (Waters, Milford, MA). Detection of atenolol in MDCKII transport samples was performed by Waters ACQUITY UPLC™ system coupled with AB Sciex 5000 triple-quadrupole mass spectrometer (AB Sciex, Foster City, CA). The samples were processed by deproteination with the same volume of acetonitrile containing appropriate internal standard. The

Downloaded from dmd.aspetjournals.org at ASPET Journals on April 19, 2024

DMD Fast Forward. Published on April 23, 2015 as DOI: 10.1124/dmd.115.064170
This article has not been copyedited and formatted. The final version may differ from this version.

chromatographic separation was achieved on a Waters ACQUITY UPLC™ BEH C18 (50 × 2.1 mm, 1.7 µm, Waters, Milford, MA) analytical column at 40°C, using a gradient of aqueous and organic mobile phase at a flow rate of 600 µL/min. Run time for each compound was 2.5 min. Key mass spectrometric settings were optimized to yield best sensitivity for each test compound. The precursor ion transitions to the strongest intensity product ions of 288.2→58.1 for zolmitriptan, 482.3→258.3 for rosuvastatin, 502.3→466.5 for fexofenadine, and 267.1→190.1 for atenolol.

Bioanalysis of triptans in in vitro HEK293 and in vivo mouse plasma, brain, and liver samples were performed by AB Sciex Qtrap 5500 mass spectrometer (AB Sciex, Foster City, CA) equipped with a Prominence UPLC system (Shimadzu, Kyoto, Japan). The chromatographic separation was achieved on a Atlantis T3 (3 µm , 2.1 mm × 50 mm WATERS , Tokyo , Japan) at 40°C using a gradient of aqueous (0.1% formic acid) and organic mobile phase (acetonitrile) a flow rate of 400 µL/min (0min, 3%; 0.3min, 3%; 2.2min, 90%; 3min, 90%; 3.1min,3%). The precursor ion transitions to the strongest intensity product ions of 296.2→157.1 for sumatriptan, 335.8→58.1 for almotriptan, 335.7→98.1 for naratriptan, 269.7→58.1 for rizatriptan, and 288.1→58.0 for zolmitriptan.

Quantitative Real-time RT-PCR

Total RNA was extracted from BacMam2-OATP1A2 transduced or non-transduced MDCKII-wild type (WT) or MDCKII-MDR1 cells using the Qiagen® RNeasy Mini kit according to the manufacturer's instructions. Human total RNA samples were purchased from Clontech (Palo Alto, CA). The RNA panel for the 18 human tissues contained different numbers of individuals

Downloaded from dmd.aspetjournals.org at ASPET Journals on April 19, 2024

DMD Fast Forward. Published on April 23, 2015 as DOI: 10.1124/dmd.115.064170
This article has not been copyedited and formatted. The final version may differ from this version.

between 14 and 68 years of age. The lowest number of individuals was 1 male or female Caucasians for brain (whole), liver, kidney and colon with mucosa, and highest number was 64 male/female Caucasians for thyroid gland. Five hundred nanograms of aforementioned RNA were reversely transcribed to cDNA in a final volume of 20 µL using the Qiagen® Omnicript RT kit.

The SYBR® Green PCR Master Mix (Applied Biosystems, Foster City, CA) was used for quantitative gene expression analysis on an ABI 7900HT Fast Real-time PCR System (Applied Biosystems, Foster City, CA) with primers as detailed in Table 1. Fifteen microliters reaction mixtures in a MicroAmp Fast Optical 384-well reaction plate (Applied Biosystems, Foster City, CA) contained 0.5 µl cDNA, 7.5 µl SYBR® Green PCR Master Mix and 75 nM forward and reverse primer. Cycling conditions were 2 min at 50°C, 10 min at 95°C, followed with 40 cycles of alternating 15 s at 95°C and 1 min at 60°C. Cycle time (Ct) values for OATP1A2, OATP2B1, P-gp and BCRP genes were first normalized with that of GAPDH in the same sample ($\Delta Ct = Ct_{OATP1A2}-Ct_{GAPDH}$), and then relative gene expression was determined by the formula $2^{-\Delta Ct}$. Relative expression fold difference of OATP1A2 as compared to other genes (BCRP, P-gp, and OATP2B1) was determined by the formula $2^{-\Delta\Delta Ct}$ ($\Delta\Delta C_t = \Delta Ct_{OATP1A2} - \Delta Ct_{other\ gene}$).

Protein Quantification of OATP1A2 by LC–MS/MS

Protein quantification of OATP1A2 in OATP1A2 transduced MDCKII membrane extracts was conducted by mass spectrometry-based targeted proteomics using validated LC–MS/MS methods. Briefly, the cells were isolated from the transwell filters using the extraction buffer I of ProteoExtract membrane extraction kit. The total membrane proteins were isolated and digested using procedure outlined before (Prasad et al., 2014). Triple-quadrupole LC-MS instrument (Xevo TQ-S coupled to ACQUITY UPLC (Waters) was used in ESI positive ionization mode.

Downloaded from dmd.aspetjournals.org at ASPET Journals on April 19, 2024

DMD Fast Forward. Published on April 23, 2015 as DOI: 10.1124/dmd.115.064170
This article has not been copyedited and formatted. The final version may differ from this version.

Approximately 2 µg of the trypsin digest (5 µL) was injected onto the column (Kinetex 1.7 µm, C18 100A; 100 × 2.1 mm, Phenomenex, Torrance, CA) and eluted at 0.3 mL/min. A mobile phase consisting of water containing 0.1% formic acid (A) and acetonitrile containing 0.1% formic acid (B) was employed. A flow rate of 0.3 mL/min was used with elution starting at 3% B for 3.0 min, followed by a linear gradient increasing to 60% B (3-20.0 min). This was followed by eluting the column with 90% mobile phase B for 0.9 min, and re-equilibrating it at 3%B for 4.9 min. MS/MS analysis was performed by monitoring the surrogate peptide (m/z 602.1 to m/z 673.8, 774.7 and 903.8) and the internal standard (606.2 to 681.7, 911.9 and 783.3) using an optimized fragmentor voltage of 33 V and collision energy of 22 eV. The LC/MS/MS data were processed by integrating the peak areas generated from the reconstructed ion chromatograms for the surrogate peptides and the internal standards using MassLynx 4.1 (Waters). The peak response for two transitions from each peptide were averaged for quantification of samples or standards. Calibrators and quality control samples were assays as before (Prasad et al., 2014). Accuracy and precision of the assay was >80% and <20% respectively. OATP1A2 protein expression data (picomoles per milligram) were expressed relative to the total protein content of the isolated membrane, as determined by the BCA assay. All samples were digested and measured in duplicate.

Data Analysis

Three-compartmental model was set up to describe the concentration-dependent and time-course of apical-to-basolateral transcellular transport of rosuvasatin (Fig. 1). The differential equations used to describe rate of mass change in apical, cellular and basolateral compartments are as follow:

$$dX_A/dt = C_C PS_A - C_A PS_A - C_A PS_{influx} \quad (1)$$

Downloaded from dmd.aspetjournals.org at ASPET Journals on April 19, 2024

DMD Fast Forward. Published on April 23, 2015 as DOI: 10.1124/dmd.115.064170
This article has not been copyedited and formatted. The final version may differ from this version.

$$dX_C/dt = C_A PS_{influx} + C_A PS_A + C_B PS_B - C_C(PS_A + PS_B) \quad (2)$$

$$dX_B/dt = C_C PS_B - C_B PS_A \quad (3)$$

where dX_A/dt, dX_B/dt, and dX_C/dt represent the substrate flux into and out of the apical, basolateral, and cellular compartments, respectively; C_A, C_B, and C_C represent substrate concentration in each compartment; PS_A and PS_B represent passive permeability-surface area product at apical and basolateral membranes and here assumes $PS_A = PS_B$; PS_{influx} represents permeability-surface area product of OATP1A2-mediated uptake activity. When substrate concentration approached or exceeded the K_m, the following equation was used:

$$PS_{influx} = V_{max}/(K_m + C_A) \quad (4)$$

Where PS_{influx} represents the permeability-surface area product of OATP1A2-mediated influx activity (μL/s); V_{max} represents maximal influx velocity (nmol/min); K_m represents the concentration of substrate when the initial transport rate is at one-half of maximum (μM); C_A represents apical donor concentration (μM). The models were constructed using SimBiology® software and the data analysis was conducted in MATLAB (version 8.4, The MathWorks, Inc.).

Assuming initial unidirectional flux into the basolateral compartment (i.e. $C_B = 0$) and rapid equilibration between apical and cellular compartments ($dX_C/dt = 0$), the flux in the apical-to-basolateral direction can be described by following equations:

$$dX_B/dt = C_C PS_B \quad (5)$$

$$C_C = (C_A PS_{influx} + C_A PS_A)/(PS_A + PS_B) \quad (6)$$

Substitution of eq. 6 into eq.5 yields the apical-to-basolateral flux equation:

$$dX_B/dt = PS_B \times (C_A PS_{influx} + C_A PS_A)/(PS_A + PS_B) \quad (7)$$

In the absence of OATP1A2 mediated influx clearance ($PS_{influx} = 0$), apical-to-basolateral flux is given by eq. 8:

Downloaded from dmd.aspetjournals.org at ASPET Journals on April 19, 2024

DMD Fast Forward. Published on April 23, 2015 as DOI: 10.1124/dmd.115.064170
This article has not been copyedited and formatted. The final version may differ from this version.

$$dX_B/dt_{\text{without OATP1A2}} = PS_B \times C_A PS_A/(PS_A + PS_B) \quad (8)$$

Under the sink condition, eq. 7 divided by eq. 8 should equate to ratio of apical-to-basolateral permeability-surface area product in presence to absence of OATP1A2 mediated influx:

$$PS_{\text{A-to-B, with OATP1A2}}/PS_{\text{A-to-B, without OATP1A2}} = 1 + PS_{\text{influx}}/PS_A \quad (9)$$

According to eq. 8, apical-to-basolateral passive permeability ($PS_{\text{A-to-B, without OATP1A2}}$) is half of PS_A under the assumption of equal apical and basolateral passive permeability ($PS_A = PS_B$). Thus, OATP1A2 mediated uptake clearance for substrate drugs across MDCKII monolayer is defined as follows:

$$PS_{\text{influx}} = 2 \times (PS_{\text{A-to-B, with OATP1A2}} - PS_{\text{A-to-B, without OATP1A2}}) \quad (10)$$

Statistical Analysis

All data are presented as mean ± standard deviation. A two-tailed Student's *t* test or one-way or two-way analysis of variance (ANOVA) followed by Tukey's multiple comparison test, where appropriate, was used to determine the statistical significance of differences among two or more groups. Linear regression analysis was performed with Microsoft Excel 2007. In all cases, $p < 0.05$ was considered to be statistically significant.

Downloaded from dmd.aspetjournals.org at ASPET Journals on April 19, 2024

DMD Fast Forward. Published on April 23, 2015 as DOI: 10.1124/dmd.115.064170
This article has not been copyedited and formatted. The final version may differ from this version.

Results

Transport of triptan drugs by Oatp1a4

Sumatriptan, naratriptan, and zolmitriptan were administered by continuous infusion up to 60 min to obtain plasma concentrations and brain- and liver-to-plasma ratios between wild-type (WT) and Oatp1a4 knock-out [Oatp1a4 (−/−)] mice. We did not observe any difference in brain- and liver-to-plasma ratios between WT and Oatp1a4 (−/−) mice at 60 min. Plasma concentrations at 30 and 60 min were similar between the two genotypes of mice (Fig. 2). These results indicated that brain and liver penetration of triptans were not impacted by Oatp1a4 in vivo.

To confirm the role Oatp1a4 played in the in vivo studies, uptake was determined in mock and mOatp1a4 transfected HEK293 cells in the absence and presence of rifampicin, a potent inhibitor of mOatp1a4. $E_2$17βG and TCA were used as positive controls. The uptake of all test triptans at 10 min was not significantly different between mock and Oatp1a4 transfected HEK293 cells (Fig. 3). Rifampicin did not influence the transport activities of triptans in mock and mOatp1a4 transfected HEK293 cells. The Oatp1a4 mediated uptake of $E_2$17βG and TCA was evident in mOatp1a4 transfected HEK293 cells and the uptake could be inhibited by rifampicin, demonstrating Oatp1a4 activity in the in vitro system.

Membrane localization of OATP1A2 in BacMam2-OATP1A2 transduced MDCKII-MDR1 cells

The membrane localization of OATP1A2 in MDCKII cells was examined by immunocytochemical staining, with P-gp used as a marker of the apical membrane of MDCKII cells. Nuclei were stained with DAPI (blue fluorescence). Both P-gp (green fluorescence) and OATP1A2 (red fluorescence) displayed an asymmetric and overlapping distribution pattern (Fig. 4). The results confirm that OATP1A2 is expressed predominantly in the apical membranes of

Downloaded from dmd.aspetjournals.org at ASPET Journals on April 19, 2024

DMD Fast Forward. Published on April 23, 2015 as DOI: 10.1124/dmd.115.064170
This article has not been copyedited and formatted. The final version may differ from this version.

the cultured MDCKII cells.

Tissue distribution of OATP1A2 mRNAs

Human brain OATP1A2 mRNA expression was comparable to BCRP and OATP2B1 and much higher than P-gp (Fig. 5A). Expression level was also significantly higher in the brain mRNA pools as compared to the other tissues evaluated, including liver, kidney and lung (Fig. 5B). Fetal brain had much lower OATP1A2 mRNA expression compared with adult human brain (Fig. 5B).

Expression of OATP1A2 and P-gp in BacMam2-OATP1A2 transduced MDCKII-WT and MDCKII-MDR1 cells

The mRNA and protein expression of OATP1A2 and mRNA expression of P-gp was characterized in OATP1A2 expressing MDCKII-WT and MDCKII-MDR1 cells. Transduction of BacMam2-OATP1A2 virus in MDCKII-MDR1 cells resulted in a proportional increase in mRNA levels of OATP1A2 with MOI up to 1000, whereas the mRNA level of OATP1A2 increased linearly with MOI up to 500 and then leveled off in MDCKII-WT cells (Fig. 6A). mRNA expression of OATP1A2 had a strong correlation with protein levels in combined both types of MDCKII cells (R^2 = 0.74, Fig. 6B). There was a trend towards human P-gp mRNA level increasing slightly with increasing MOI of BacMam2-OATP1A2 virus in MDCKII-MDR1 (Fig. 6C). Virus transduction led to a decrease of endogenous canine P-gp in MDCKII-WT cells, whereas it did not affect the expression of canine P-gp in MDCKII-MDR1 cells. MDCKII-WT cells had higher endogenous canine P-gp expression compared to MDCKII-MDR1 cells (Fig. 6D).

Monolayer integrity post BacMam2-OATP1A2 transduction

Introduction of BacMam2 virus to the Transwell apical compartment did not compromise the integrity of MDCKII cells up to MOI of 1000, as indicated by low permeability of paracellular

Downloaded from dmd.aspetjournals.org at ASPET Journals on April 19, 2024

DMD Fast Forward. Published on April 23, 2015 as DOI: 10.1124/dmd.115.064170
This article has not been copyedited and formatted. The final version may differ from this version.

markers (lucifer yellow and atenolol). BacMam2 virus caused ~40% of monolayers to be leaky in MDCKII-WT cells at MOI of 2000, whereas it had less effect in MDCKII-MDR1 cells. Resultant data from monolayers transduced with BacMam2-OATP1A2 at MOI of 2000 were excluded from further analysis, due to loss of monolayer integrity. Interestingly, TEER values of MDCKII monolayers increased with increasing MOI of BacMam2-OATP1A2 viruses (Fig. 7A and 7B). Apical-to-basolateral or basolateral-to-apical permeability of the paracellular marker atenolol did not change substantially with MOI of BacMam viruses in MDCKII-WT and MDCKII-MDR1 monolayers (Fig. 7C and 7D). We observed a trend of increasing apical-to-basolateral permeability of atenolol with corresponding increases in expression of OATP1A2 in MDCKII-WT cells. However, data variability and lack of correlation between atenolol and lucifer yellow permeability in these wells precluded us to making a definite conclusion. The impact on permeability of zolmitriptan and rosuvastatin was expected to be minimal, since their permeability was at least two-fold higher in the OATP1A2 transfected cells.

Transcellular transport of zolmitriptan, rosuvastatin, and fexofenadine across OATP1A2 expressing MDCKII-WT and MDCKII-MDR1 monolayers

Bidirectional transcellular permeability of zolmitriptan, rosuvastatin and fexofenadine was examined in MDCKII-WT and MDCKII-MDR1 monolayers expressing different levels of OATP1A2. Apical-to-basolateral transcellular permeability increased with increasing protein expression level of OATP1A2 in the two types of MDCKII cells (Fig. 8). The efflux ratio of zolmitriptan and fexofenadine was 7.7 and 3.3 in MDCKII-MDR1 cells, respectively and 1.1 and 3.2 in MDCKII-WT cells, suggesting these are P-gp substrates in line with previous reports (Cvetkovic et al., 1999; Evans et al., 2003). The efflux ratios of zolmitriptan and fexofenadine at protein expression of OATP1A2 at 0.17 fmol/µg protein were 0.21 and 0.53 in MDCKII-WT

Downloaded from dmd.aspetjournals.org at ASPET Journals on April 19, 2024

DMD Fast Forward. Published on April 23, 2015 as DOI: 10.1124/dmd.115.064170
This article has not been copyedited and formatted. The final version may differ from this version.

cells and 0.43 and 1.6 in MDCKII-MDR1 cells, respectively, suggesting that OATP1A2 counteracted P-gp efflux effects for co-substrates. Rosuvastatin is not a P-gp substrate, as indicated by efflux ratios of 1.2 in MDCKII-WT and 1.4 in MDCKII-MDR1 cells. The efflux ratio of rosuvastatin at OATP1A2 protein expression of 0.17 fmol/µg protein was 0.06 in MDCKII-WT cells and 0.09 in MDCKII-MDR1 cells respectively, exhibiting no substantial difference in the two cell types. Virus transduction did not change the permeability of midazolam (data not shown here), a non-OATP1A2 substrate that we evaluated previously (Cheng et al., 2012). OATP1A2 mediated uptake clearance was calculated using eq. 10 for zolmitriptan in MDCKII-WT cells and rosuvastatin in both cell types because their transport was not affected by P-gp in these cells. The uptake clearance was directly proportional to the protein levels of OATP1A2 (Fig. 9). The coefficient of correlation (R^2) was strong for zolmitriptan in MDCKII-WT cells (0.94, $p < 0.01$) and rosuvastatin in MDCKII-MDR1 cells (0.96, $p < 0.01$). The correlation was weaker and not statistically significant for rosuvastatin in MDCKII-WT cells ($R^2 = 0.54$, $p = 0.16$).

Kinetic characterization of transcellular transport of Rosuvastatin across OATP1A2 expressing MDCKII-WT monolayers

Rosuvastatin is a BCRP and not a P-gp substrate (Huang et al., 2006). Since endogenous canine Bcrp expression was not detectable in our MDCKII cells (data not shown), rosuvastatin was an ideal tool compound to investigate the role of OATP1A2 in transcellular transport in a quantitative manner. To understand more mechanistically the effect of drug concentration on OATP1A2-mediated transcellular transport, apical-to-basolateral permeability of rosuvastatin was examined at concentrations between 0.3 to 300 µM and found to be high and constant at less than 10 µM. Permeability decreased with an increase in concentrations, suggesting

Downloaded from dmd.aspetjournals.org at ASPET Journals on April 19, 2024

DMD Fast Forward. Published on April 23, 2015 as DOI: 10.1124/dmd.115.064170
This article has not been copyedited and formatted. The final version may differ from this version.

saturation of OATP1A2-mediated influx. Permeability decreased in the presence of the OATP1A2 inhibitor, naringin at 500 μM (Fig. 10A). Transcellular apical-to-basolateral permeability was inhibited ~90% in the presence of naringin at low non-saturable donor concentrations (0.3 and 1 μM). The concentration-dependent apical-to-basolateral permeability of rosuvastatin was fitted using the 3-compartment model described in Fig 1 and correlated well with the observed permeability. The optimized transport kinetic parameters K_m, V_{max} and passive permeability were 30.6 μM, 0.02 nmol/min, and 2.2 nm/s, respectively (Fig. 10B). The resultant OATP1A2-mediated intrinsic transport capacity (V_{max}/K_m) was 10.9 nL/s, which corresponded to 332 nm/s, assuming 0.33 cm^2 of Transwell surface area. The concentration of rosuvastatin over time across MDCKII-WT monolayer expressing the same level of OATP1A2 could be predicted by the three-compartment model using the above-fitted kinetic parameters (Fig. 10C), further demonstrating the validity of 3-compartment model to quantitatively depict the OATP1A2-mediated transcellular transport of rosuvastatin across the polarized tight barrier.

Downloaded from dmd.aspetjournals.org at ASPET Journals on April 19, 2024

DMD Fast Forward. Published on April 23, 2015 as DOI: 10.1124/dmd.115.064170
This article has not been copyedited and formatted. The final version may differ from this version.

Discussion

OATP1A2 is highly expressed in the apical membrane of human BBB, suggesting the potential to be targeted for CNS drug delivery. At this time we lack the appropriate in vitro and in vivo tools to investigate the role of this transporter in brain penetration of xenobiotics. We have successfully constructed a versatile in vitro system using the BacMam virus to transiently express OATP1A2 in MDCKII monolayers and used this to examine the effect of OATP1A2 expression and the interplay with P-gp, on transcellular transport of substrate drugs.

OATP1A2 was identified to have high mRNA expression in human brain (Kullak-Ublick et al., 1995) and this finding was later corroborated (Eechoute et al., 2011). We examined additional transporters in mRNA preparations from whole adult human brains and report comparable OATP1A2 expression relative to BCRP and OATP2B1 and much higher expression than P-gp.

Protein expression of OATP1A2 has been reported in human brain capillaries by immunostaining (Bronger et al., 2005; Gao et al., 2000; Lee et al., 2005) and quantitated in healthy brain tissue by LC-MS/MS at 0.25 fmol/µg protein (Drozdzik et al., 2014). This is the concentration we achieved in our transduced cell lines, that lead to greatly enhanced transcellular permeability of substrate drugs. The protein expression of OATP1A2 in purified human brain microvessels may be lower than 0.695 fmol/µg protein, as Uchida et al. (2011b) could not detect the protein in purified human brain microvessels by LC-MS/MS, with this sensitivity limit.

During CNS drug discovery, mouse or rat brains are routinely analyzed to check for penetration of discovery compounds, and along with human P-gp in vitro efflux data, used to make predictions of clinical CNS distribution. P-gp is an important transporter limiting CNS penetration and is similar between the species, unlike the less homologous uptake transporters e.g. OATP1A2 and Oatp1a4 (Feng et al., 2008; Bleasby et al., 2006). Oatp1a4 is highly enriched

Downloaded from dmd.aspetjournals.org at ASPET Journals on April 19, 2024

DMD Fast Forward. Published on April 23, 2015 as DOI: 10.1124/dmd.115.064170
This article has not been copyedited and formatted. The final version may differ from this version.

in brain capillaries (Liu et al., 2014), with protein levels of 2.11 fmol/µg protein in purified mouse and rat brain microvessels (Kamiie et al., 2008). The presence of Oatp1a4 at both brain and blood side of rodent BBB could imply a role divergent from the apically expressed OATP1A2 (Bronger et al., 2005; Ose et al., 2010). As would be expected, OATP1A2 has some overlapping substrate specificity with Oatp1a4 e.g. rocuronium, fexofenadine, estrone-3-sulfate and thyroid hormone (Hagenbuch et al., 2002). However, OATP1A2 transports compounds, e.g. deltorphin II and microcystin, that are not substrates of Oatp1a4, while Leu-enkephalin and digoxin are Oatp1a4 specific substrates (Hagenbuch et al., 2002). We now report additional differences in substrate specificity with triptan drugs. The CNS penetration of systemically administered ^{14}C-labeled sumatriptan, a relatively hydrophilic triptan, was investigated in mice and only 0.006% of total radioactivity was recovered in the brain (Humphrey et al., 1990), indicating this drug was not a CNS penetrant. Similarly, sumatriptan was not found in the rat brain in whole body autoradiography studies (Dixon et al., 1993). However, in a positron emission tomography study in six migraine patients, subcutaneous sumatriptan (6 mg) normalized the migraine attack-related increases in brain serotonin synthesis (Sakai et al., 2008), demonstrating central efficacy of sumatriptan and potential brain uptake. We found that sumitriptan was an OATP1A2 substrate (Cheng et al., 2012) and this likely contributed to the species difference. Zolmitriptan is another example of a P-gp substrate that is brain penetrable, as evidenced by a clinical PET study with brain-to-blood ratio at ~0.25 (Bergstrom et al., 2006). We found this to be an OATP1A2 substrate as well (Cheng et al., 2012). We have now demonstrated in vitro and in vivo, that triptans are not substrates for Oatp1a4 and that by not factoring in potential uptake transport, we may be not progressing potentially brain penetrant compounds to the clinic. To further evaluate this, we have developed a unique in vitro MDCK model to

Downloaded from dmd.aspetjournals.org at ASPET Journals on April 19, 2024

DMD Fast Forward. Published on April 23, 2015 as DOI: 10.1124/dmd.115.064170
This article has not been copyedited and formatted. The final version may differ from this version.

investigate OATP1A2-facilitated transcellular transport.

OATP1A2 expression co-localized with P-gp in MDCKII cells, similar to the reported physiological apical localization at human BBB. The increase in apical-to-basolateral transcellular transport of zolmitriptan, rosuvastatin, and fexofenadine was consistent with the increasing OATP1A2 protein levels. OATP1A2 mediated uptake clearance was proportional to protein levels of OATP1A2. These data could support future endeavors in extrapolation of the in vitro findings to in vivo, by correcting for the difference in OATP1A2 expression levels. Of note, the basolateral-to-apical permeability of zolmitriptan and fexofenadine in MDCKII-MDR1 cells also increased with increasing OATP1A2 protein expression. This could be caused in part by increased human P-gp expression and activity after BacMam virus transduction, as immunocytochemical staining confirmed OATP1A2 not being expressed at the basolateral membrane. At the same OATP1A2 protein expression, efflux ratios of the OATP1A2 and P-gp co-substrates zolmitriptan and fexofenadine were lower in MDCKII-WT cells as compared with MDCKII-MDR1 cells. This indicates that OATP1A2 counteracts P-gp efflux effect of dual co-substrates. We used rosuvastatin as a model compound to illustrate quantitatively the contribution of OATP1A2-mediated transcellular transport across MDCKII monolayers because it is not a P-gp substrate. OATP1A2 mediated influx contributed to ~90% of apical-to-basolateral transcellular permeability of rosuvastatin across MDCKII monolayer at the expression level used in the experiment. The 3-compartment model incorporating OATP1A2 mediated influx, quantitatively described the concentration-dependent apical-to-basolateral transcellular permeability across OATP1A2 expressing MDCKII-WT monolayers. The fitted intrinsic transport capacity (V_{max}/K_m) was much larger than passive clearance, indicating substantial contribution of OATP1A2 mediated influx to transcellular permeability of rosuvastatin across

Downloaded from dmd.aspetjournals.org at ASPET Journals on April 19, 2024

DMD Fast Forward. Published on April 23, 2015 as DOI: 10.1124/dmd.115.064170
This article has not been copyedited and formatted. The final version may differ from this version.

MDCKII-WT monolayers. Since P-gp and BCRP, along with OATP1A2, are expressed at human BBB (Kalvass et al., 2013), these likely work in concert to determine the transcellular permeability across the barrier for co-substrates such as zolmitriptan and rosuvastatin.

OATP1A2 is an attractive target for enhancing brain penetration because of broad substrate specificity, desirable expression level (at least of mRNA), BBB localization, and our data indicate that this could potentially be leveraged to counteract P-gp efflux. Accurate and robust quantification of the OATP1A2 protein with membrane extracts of highly purified human brain capillaries will help this further. The physiological expression data would help us to contextualize the current in vitro findings as has previously been done for P-gp (Uchida et al., 2011a; Uchida et al., 2014). The data could also shed light on emerging debate on neuronal (Gao et al., 2014) and more widely accepted brain endothelial localization (Bronger et al., 2005; Gao et al., 2000; Kalvass et al., 2013; Lee et al., 2005).

In conclusion, we have successfully constructed OATP1A2 expressing MDCKII monolayers using a BacMam virus system and demonstrated enhanced apical-to-basolateral transcellular permeability in an OATP1A2 expression level-dependent manner. OATP1A2 mediated uptake clearance was proportional to protein levels of OATP1A2. Presence of OATP1A2 in MDCKII-MDR1 cells counteracts the efflux effect of P-gp for their co-substrates. The 3-compartmental model incorporating OATP1A2-mediated influx can quantitatively describe the concentration-dependent or time-course apical-to-basolateral transcellular transport across OATP1A2 expressing MDCKII monolayers. In spite of significant knowledge gaps for this transporter in CNS distribution, our efforts and this model represent a step forward to improve this understanding.

Downloaded from dmd.aspetjournals.org at ASPET Journals on April 19, 2024

DMD Fast Forward. Published on April 23, 2015 as DOI: 10.1124/dmd.115.064170
This article has not been copyedited and formatted. The final version may differ from this version.

Acknowledgements

The authors would like to acknowledge Dan Pu and Yiwen Wu for bioanalytical support. We also thank Chen-Bing Guan for providing technical help with immunocytochemical staining. We thank Maciej Zamek-Gliszczynski and David Tattersall for their critical review and helpful discussion during the preparation of the manuscript.

Downloaded from dmd.aspetjournals.org at ASPET Journals on April 19, 2024

DMD Fast Forward. Published on April 23, 2015 as DOI: 10.1124/dmd.115.064170
This article has not been copyedited and formatted. The final version may differ from this version.

Authorship Contributions

Participated in research design: Liu, Unadkat, Kusuhara, Sugiyama, Sahi.

Conducted experiments: Liu, Yu, Lu S, Ito, Zhang, Prasad, Lu X, Li, Wang.

Contributed new reagents or analytical tools: An, Xu, Prasad, Unadkat.

Performed data analysis: Liu, Yu, Lu S, Ito, Zhang, He, Lu X, Kusuhara.

Wrote or contributed to the writing of the manuscript: Liu, Prasad, Unadkat, Kusuhara, Sahi.

Downloaded from dmd.aspetjournals.org at ASPET Journals on April 19, 2024

DMD Fast Forward. Published on April 23, 2015 as DOI: 10.1124/dmd.115.064170
This article has not been copyedited and formatted. The final version may differ from this version.

References

Badagnani I, Castro RA, Taylor TR, Brett CM, Huang CC, Stryke D, Kawamoto M, Johns SJ, Ferrin TE, Carlson EJ, Burchard EG and Giacomini KM (2006) Interaction of methotrexate with organic-anion transporting polypeptide 1A2 and its genetic variants. *J Pharmacol Exp Ther* **318**:521-529.

Bergstrom M, Yates R, Wall A, Kagedal M, Syvanen S and Langstrom B (2006) Blood-brain barrier penetration of zolmitriptan--modelling of positron emission tomography data. *J Pharmacokinet Pharmacodyn* **33**:75-91.

Bleasby K, Castle JC, Roberts CJ, Cheng C, Bailey WJ, Sina JF, Kulkarni AV, Hafey MJ, Evers R, Johnson JM, Ulrich RG and Slatter JG (2006) Expression profiles of 50 xenobiotic transporter genes in humans and pre-clinical species: a resource for investigations into drug disposition. *Xenobiotica* **36**:963-988.

Bourasset F, Cisternino S, Temsamani J and Scherrmann JM (2003) Evidence for an active transport of morphine-6-beta-d-glucuronide but not P-glycoprotein-mediated at the blood-brain barrier. *J Neurochem* **86**:1564-1567.

Bronger H, Konig J, Kopplow K, Steiner HH, Ahmadi R, Herold-Mende C, Keppler D and Nies AT (2005) ABCC drug efflux pumps and organic anion uptake transporters in human gliomas and the blood-tumor barrier. *Cancer Res* **65**:11419-11428.

Cheng Z, Liu H, Yu N, Wang F, An G, Xu Y, Liu Q, Guan CB and Ayrton A (2012) Hydrophilic anti-migraine triptans are substrates for OATP1A2, a transporter expressed at human blood-brain barrier. *Xenobiotica* **42**:880-890.

Cheng X, Maher J, Chen C and Klaassen CD (2005) Tissue distribution and ontogeny of mouse organic anion transporting polypeptides (Oatps). *Drug Metab Dispos* **33:**1062-1073.

Ciurleo R, Bramanti P and Marino S (2014) Role of statins in the treatment of multiple sclerosis. *Pharmacol Res* **87**:133-143.

Cvetkovic M, Leake B, Fromm MF, Wilkinson GR and Kim RB (1999) OATP and P-glycoprotein transporters mediate the cellular uptake and excretion of fexofenadine. *Drug Metab Dispos* **27**:866-871.

Dixon CM, Saynor DA, Andrew PD, Oxford J, Bradbury A and Tarbit MH (1993) Disposition of sumatriptan in laboratory animals and humans. *Drug Metab Dispos* **21**:761-769.

Drozdzik M, Groer C, Penski J, Lapczuk J, Ostrowski M, Lai Y, Prasad B, Unadkat JD, Siegmund W and Oswald S (2014) Protein abundance of clinically relevant multidrug transporters along the entire length of the human intestine. *Mol Pharm* **11**:3547-3555.

Eechoute K, Franke RM, Loos WJ, Scherkenbach LA, Boere I, Verweij J, Gurney H, Kim RB, Tirona RG, Mathijssen RH and Sparreboom A (2011) Environmental and genetic factors affecting transport of imatinib by OATP1A2. *Clin Pharmacol Ther* **89**:816-820.

Evans DC, O'Connor D, Lake BG, Evers R, Allen C and Hargreaves R (2003) Eletriptan metabolism by human hepatic CYP450 enzymes and transport by human P-glycoprotein. *Drug Metab Dispos* **31**:861-869.

Feng B, Mills JB, Davidson RE, Mireles RJ, Janiszewski JS, Troutman MD and de Morais SM (2008) In vitro P-glycoprotein assays to predict the in vivo interactions of P-glycoprotein with drugs in the central nervous system. *Drug Metab Dispos* **36**:268-275.

Fonfara S, Hetzel U, Tew SR, Dukes-McEwan J, Cripps P and Clegg PD (2011) Leptin expression in dogs with cardiac disease and congestive heart failure. *J Vet Intern Med* **25**:1017-1024.

Franke RM, Scherkenbach LA and Sparreboom A (2009) Pharmacogenetics of the organic anion transporting polypeptide 1A2. *Pharmacogenomics* **10**:339-344.

Gao B, Hagenbuch B, Kullak-Ublick GA, Benke D, Aguzzi A and Meier PJ (2000) Organic anion-transporting polypeptides mediate transport of opioid peptides across blood-brain barrier. *J Pharmacol Exp Ther* **294**:73-79.

Gao B, Stieger B, Noe B, Fritschy JM and Meier PJ (1999) Localization of the organic anion transporting polypeptide 2 (Oatp2) in capillary endothelium and choroid plexus epithelium of rat brain. *J Histochem Cytochem* **47**:1255-1264.

Gao B, Vavricka SR, Meier PJ and Stieger B (2014) Differential cellular expression of organic anion transporting peptides OATP1A2 and OATP2B1 in the human retina and brain: implications for carrier-mediated transport of neuropeptides and neurosteriods in the CNS. *Pflugers Arch* doi: 10.1007/s00424-014-1596-x.

Glaeser H, Bailey DG, Dresser GK, Gregor JC, Schwarz UI, McGrath JS, Jolicoeur E, Lee W, Leake BF, Tirona RG and Kim RB (2007) Intestinal drug transporter expression and the impact of grapefruit juice in humans. *Clin Pharmacol Ther* **81**:362-370.

Hagenbuch B, Gao B and Meier PJ (2002) Transport of xenobiotics across the blood-brain barrier. *News Physiol Sci*

Downloaded from dmd.aspetjournals.org at ASPET Journals on April 19, 2024

DMD Fast Forward. Published on April 23, 2015 as DOI: 10.1124/dmd.115.064170
This article has not been copyedited and formatted. The final version may differ from this version.

17:231-234.
Horibe S, Nagai J, Yumoto R, Tawa R and Takano M (2011) Accumulation and photodynamic activity of chlorin e6 in cisplatin-resistant human lung cancer cells. *J Pharm Sci* **100**:3010-3017.
Hsiao P and Unadkat JD (2014) Predicting the outer boundaries of P-glycoprotein (P-gp)-based drug interactions at the human blood-brain barrier based on rat studies. *Mol Pharm* **11**:436-444.
Huang L, Wang Y and Grimm S (2006) ATP-dependent transport of rosuvastatin in membrane vesicles expressing breast cancer resistance protein. *Drug Metab Dispos* **34**:738-742.
Humphrey PP, Feniuk W, Perren MJ, Beresford IJ, Skingle M and Whalley ET (1990) Serotonin and migraine. *Ann N Y Acad Sci* **600**:587-598; discussion 598-600.
Kalvass JC, Polli JW, Bourdet DL, Feng B, Huang SM, Liu X, Smith QR, Zhang LK, Zamek-Gliszczynski MJ and International Transporter C (2013) Why clinical modulation of efflux transport at the human blood-brain barrier is unlikely: the ITC evidence-based position. *Clin Pharmacol Ther* **94**:80-94.
Kamiie J, Ohtsuki S, Iwase R, Ohmine K, Katsukura Y, Yanai K, Sekine Y, Uchida Y, Ito S and Terasaki T (2008) Quantitative atlas of membrane transporter proteins: development and application of a highly sensitive simultaneous LC/MS/MS method combined with novel in-silico peptide selection criteria. *Pharm Res* **25**:1469-1483.
Kikuchi R, Kusuhara H, Abe T, Endou H and Sugiyama Y (2004) Involvement of multiple transporters in the efflux of 3-hydroxy-3-methylglutaryl-CoA reductase inhibitors across the blood-brain barrier. *J Pharmacol Exp Ther* **311**:1147-1153.
Kullak-Ublick GA, Hagenbuch B, Stieger B, Schteingart CD, Hofmann AF, Wolkoff AW and Meier PJ (1995) Molecular and functional characterization of an organic anion transporting polypeptide cloned from human liver. *Gastroenterology* **109**:1274-1282.
Kuteykin-Teplyakov K, Luna-Tortos C, Ambroziak K and Loscher W (2010) Differences in the expression of endogenous efflux transporters in MDR1-transfected versus wildtype cell lines affect P-glycoprotein mediated drug transport. *Br J Pharmacol* **160**:1453-1463.
Lee W, Glaeser H, Smith LH, Roberts RL, Moeckel GW, Gervasini G, Leake BF and Kim RB (2005) Polymorphisms in human organic anion-transporting polypeptide 1A2 (OATP1A2): implications for altered drug disposition and central nervous system drug entry. *J Biol Chem* **280**:9610-9617.
Liu H, Li Y, Lu S, Wu Y and Sahi J (2014) Temporal expression of transporters and receptors in a rat primary co-culture blood-brain barrier model. *Xenobiotica* **44**:941-951.
Maeda T, Takahashi K, Ohtsu N, Oguma T, Ohnishi T, Atsumi R and Tamai I (2007) Identification of influx transporter for the quinolone antibacterial agent levofloxacin. *Mol Pharm* **4**:85-94.
Mayerl S, Visser TJ, Darras VM, Horn S and Heuer H (2012) Impact of Oatp1c1 deficiency on thyroid hormone metabolism and action in the mouse brain. *Endocrinology* **153:**1528-1537.
Maubon N, Le Vee M, Fossati L, Audry M, Le Ferrec E, Bolze S and Fardel O (2007) Analysis of drug transporter expression in human intestinal Caco-2 cells by real-time PCR. *Fundam Clin Pharmacol* **21**:659-663.
Ose A, Kusuhara H, Endo C, Tohyama K, Miyajima M, Kitamura S and Sugiyama Y (2010) Functional characterization of mouse organic anion transporting peptide 1a4 in the uptake and efflux of drugs across the blood-brain barrier. *Drug Metab Dispos* **38**:168-176.
Prasad B, Evers R, Gupta A, Hop CE, Salphati L, Shukla S, Ambudkar SV and Unadkat JD (2014) Interindividual variability in hepatic organic anion-transporting polypeptides and P-glycoprotein (ABCB1) protein expression: quantification by liquid chromatography tandem mass spectroscopy and influence of genotype, age, and sex. *Drug Metab Dispos* **42**:78-88.
Rautio J, Humphreys JE, Webster LO, Balakrishnan A, Keogh JP, Kunta JR, Serabjit-Singh CJ and Polli JW (2006) In vitro p-glycoprotein inhibition assays for assessment of clinical drug interaction potential of new drug candidates: a recommendation for probe substrates. *Drug Metab Dispos* **34**:786-792.
Ronaldson PT, Finch JD, Demarco KM, Quigley CE and Davis TP (2011) Inflammatory pain signals an increase in functional expression of organic anion transporting polypeptide 1a4 at the blood-brain barrier. *J Pharmacol Exp Ther* **336**:827-839.
Sakai Y, Dobson C, Diksic M, Aube M and Hamel E (2008) Sumatriptan normalizes the migraine attack-related increase in brain serotonin synthesis. *Neurology* **70**:431-439.
Sierra S, Ramos MC, Molina P, Esteo C, Vazquez JA and Burgos JS (2011) Statins as neuroprotectants: a comparative in vitro study of lipophilicity, blood-brain-barrier penetration, lowering of brain cholesterol, and decrease of neuron cell death. *J Alzheimers Dis* **23**:307-318.
Taogoshi T, Nomura A, Murakami T, Nagai J and Takano M (2005) Transport of prostaglandin E1 across the blood-brain barrier in rats. *J Pharm Pharmacol* **57**:61-66.

Downloaded from dmd.aspetjournals.org at ASPET Journals on April 19, 2024

DMD Fast Forward. Published on April 23, 2015 as DOI: 10.1124/dmd.115.064170
This article has not been copyedited and formatted. The final version may differ from this version.

Tran TT, Mittal A, Gales T, Maleeff B, Aldinger T, Polli JW, Ayrton A, Ellens H and Bentz J (2004) Exact kinetic analysis of passive transport across a polarized confluent MDCK cell monolayer modeled as a single barrier. *J Pharm Sci* **93**:2108-2123.

Uchida Y, Ohtsuki S, Kamiie J and Terasaki T (2011a) Blood-brain barrier (BBB) pharmacoproteomics: reconstruction of in vivo brain distribution of 11 P-glycoprotein substrates based on the BBB transporter protein concentration, in vitro intrinsic transport activity, and unbound fraction in plasma and brain in mice. *J Pharmacol Exp Ther* **339**:579-588.

Uchida Y, Ohtsuki S, Katsukura Y, Ikeda C, Suzuki T, Kamiie J and Terasaki T (2011b) Quantitative targeted absolute proteomics of human blood-brain barrier transporters and receptors. *J Neurochem* **117**:333-345.

Uchida Y, Wakayama K, Ohtsuki S, Chiba M, Ohe T, Ishii Y and Terasaki T (2014) Blood-brain barrier pharmacoproteomics-based reconstruction of the in vivo brain distribution of P-glycoprotein substrates in cynomolgus monkeys. *J Pharmacol Exp Ther* **350**:578-588.

Urquhart BL and Kim RB (2009) Blood-brain barrier transporters and response to CNS-active drugs. *Eur J Clin Pharmacol* **65**:1063-1070.

Wang J, Guo LP, Chen LZ, Zeng YX and Lu SH (2007) Identification of cancer stem cell-like side population cells in human nasopharyngeal carcinoma cell line. *Cancer Res* **67**:3716-3724.

Downloaded from dmd.aspetjournals.org at ASPET Journals on April 19, 2024

DMD Fast Forward. Published on April 23, 2015 as DOI: 10.1124/dmd.115.064170
This article has not been copyedited and formatted. The final version may differ from this version.

Footnotes

Na Yu was recruited by GSK as a student intern from Shanghai Jiaotong University when the work was conducted. This work was presented in part as a poster presentation at the CPSA, Shanghai, China, April 17–18, 2014: Na Yu *et al*. OATP1A2 and P-gp Expression Level Dependent Transport of Zolmitriptan and Fexofenadine Across MDCKII Monolayers.

Downloaded from dmd.aspetjournals.org at ASPET Journals on April 19, 2024

DMD Fast Forward. Published on April 23, 2015 as DOI: 10.1124/dmd.115.064170
This article has not been copyedited and formatted. The final version may differ from this version.

Figure Legends:

Fig. 1. Schematic of the three-compartment model to describe OATP1A2-mediated transcellular transport across the MDCKII cell monolayer. PS_A and PS_B: passive permeability-surface area product at apical and basolateral membranes, respectively; PS_{influx}: permeability-surface area product of OATP1A2-mediated uptake activity; C_A, C_B, and C_C represent substrate concentration in apical, basolateral, and cellular compartments, respectively.

Fig. 2. Comparison of brain and liver uptake of triptan drugs. Sumatriptan (A), naratriptan (B), and zolmitriptan (C) were administered to wild-type (WT, open box) and Oatp1a4(–/–) knock-out (KO, filled box) mice via constant iv infusion, as described in METHODS. Blood samples were collected from jugular vein at 30 and 60 min after treatment, brain and liver were excised at 60 min and plasma obtained by centrifugation of blood samples. Concentrations of sumatriptan, naratriptan, and zolmitriptan were determined with LC-MS/MS analysis. Differences in brain/plasma and liver/plasma ratios between wild-type and Oatp1a4(–/–) mice for sumatriptan, naratriptan, and zolmitriptan was assessed by a two-tailed Student's t test and were not statistically significant.

Fig. 3. Uptake of almotriptan, zolmitriptan, sumatriptan, rizatriptan, and naratriptan by mock or Oatp1a4 transfected HEK293 cells. These experiments were conducted in the absence and presence of rifampicin (100 μM), in triplicate for triptans (1 μM for 10 min) and the positive controls [^{3}H]$E_2$17βG and [^{3}H]TCA (1 μM for 5 min) as per experimental protocols described in **Methods**. Statistical significance was assessed by one-way analysis of variance followed by Tukey's multiple comparison test. ***, $P < 0.001$, statistically different uptake between empty-vector and Oatp1a4 transfected HEK293 cells. †††, $P < 0.001$, statistically different uptake between absence and presense of rifampicin in Oatp1a4 transfected HEK293 cells.

Downloaded from dmd.aspetjournals.org at ASPET Journals on April 19, 2024

DMD Fast Forward. Published on April 23, 2015 as DOI: 10.1124/dmd.115.064170
This article has not been copyedited and formatted. The final version may differ from this version.

Fig. 4. Membrane localization of human OATP1A2 and P-gp in Bacmam2-OATP1A2 transduced MDCKII-MDR1 cells. (A) MDCKII-MDR1 cells transduced with BacMam2-OATP1A2 virus were stained with monoclonal antibodies against OATP1A2 (red fluorescence) and human P-gp (green fluorescence). Nuclei were stained with DAPI (blue fluorescence). Pictures are single optical sections (X/Y) (center) with X/Z (bottom) and Y/Z (right) projections, respectively. Apical and basolateral sides of MDCKII-MDR1 cells are at positions indicated in X/Z (bottom) and Y/Z (right) projections. Dotted line indicates the position where Y-Z and X-Z images locate. Scale = 10 μm (in X-Y image). (B) Normalized fluorescent intensity profiles of OATP1A2, P-gp and DAPI along the lines from apical to basal sides (indicated by white arrows) from four representative cells selected from the Y-Z or X-Z images (indicated by dashed rectangles in A).

Fig. 5. mRNA expression of OATP1A2 across different human tissues. mRNA expression of OATP1A2 was normalized to (A) P-gp, BCRP, and OATP2B1 in human brain and cerebellum and (B) GAPDH across different human tissues. Expression levels were analyzed in triplicate.

Fig. 6. Transporter mRNA expression after Bacmam transduction. Expression of OATP1A2 (A), human P-gp (C) and canine P-gp (D) in MDCKII-WT (■) and MDCKII-MDR1 (●) cells after transduction of BacMam2-OATP1A2 with increasing multiplicity of infection (MOI), up to 1000. Correlation between mRNA and protein levels of OATP1A2 in the two cell types transduced by BacMam2-OATP1A2 (B).

Fig. 7. Monolayer integrity of MDCKII-WT and MDCKII-MDR1 monolayers after transduction of BacMam2-OATP1A2 with increasing MOI up to 1000. TEER values of WT (A) and MDR1 (B) cells (n = 24-48); Apical-to-basolateral (●) or basolateral-to-apical (▲) permeability of paracellular marker atenolol with MOI of BacMam viruses in MDCKII-WT (C) and MDCKII-

Downloaded from dmd.aspetjournals.org at ASPET Journals on April 19, 2024

DMD Fast Forward. Published on April 23, 2015 as DOI: 10.1124/dmd.115.064170
This article has not been copyedited and formatted. The final version may differ from this version.

MDR1 (D) monolayers. Transport experiment for atenolol was conducted with 3 μM for 90 min, in triplicate.

Fig. 8. Permeability as a function of OATP1A2 protein expression. Apical-to-basolateral (●) or basolateral-to-apical (▲) permeability of zolmitriptan (A-B), rosuvastatin (C-D) and fexofenadine (E-F) as a function of protein expression of OATP1A2 in membrane extracts of MDCKII-WT and MDCKII-MDR1 cells transduced with different titres of BacMam2-OATP1A2. Transport experiment was conducted with 1 μM compound for 90 min in triplicate.

Fig. 9. Correlation between expression levels of OATP1A2 and influx clearance (PS_{influx}) of zolmitriptan in MDCKII-WT cells (A) and rosuvastatin in MDCKII-WT (B) and MDCKII-MDR1 (C) cells. Protein level of OATP1A2 in MDCKII-MDR1 cells was taken as zero when it was below the limit of quantification (0.08 fmol/μg protein).

Fig. 10. Kinetics of transcellular transport of rosuvastatin across OATP1A2 expressing MDCKII-WT monolayers. (A) Apical-to-basolateral transcellular permeability in the absence and presence of OATP1A2 inhibitor, naringin, at 500 μM. (B) Observed concentration-dependent apical-to-basolateral permeability of rosuvastatin was fit by the 3-compartment model described in Fig. 1. (C) The resultant model parameters were used to predict the concentrations of rosuvastatin in apical and basolateral compartments over time after dosing 1 μM of rosuvastatin in apical compartment. The transport experiment was conducted in triplicate or quadruplicate. The OATP1A2 mRNA expression level normalized to *GADPH* was 0.342 in MDCKII cells used in this experiment, which OATP1A2 protein level was predicted to be 0.13 fmol/mg protein based on relationship shown in Fig. 6B.

Downloaded from dmd.aspetjournals.org at ASPET Journals on April 19, 2024

DMD Fast Forward. Published on April 23, 2015 as DOI: 10.1124/dmd.115.064170
This article has not been copyedited and formatted. The final version may differ from this version.

TABLE 1
Nucleotide sequences of primers used in real-time quantitative PCR.

Gene	Forward primer (5'−3')	Reverse primer (3'−5')	Primer reference
OATP1A2	AAGACCAACGCAGGATCCAT	GAGTTTCACCCATTCCACGTACA	(Glaeser et al., 2007)
OATP2B1	CTTCATCTCGGAGCCATACC	GCTTGAGCAGTTGCCATTG	(Glaeser et al., 2007)
Human P-gp	GCCAAAGCCAAAATATCAGC	TTCCAATGTGTTCGGCAT	(Maubon et al., 2007)
Canine P-gp	TTGCTGGTTTTGATGATGGA	CTGGACCCTGAATCTTTTGG	(Kuteykin-Teplyakov et al., 2010)
Human BCRP	GGATGAGCCTACAACTGGCTT	CTTCCTGAGGCCAATAAGGTG	(Horibe et al., 2011)
Human GADPH	GAGTCAACGGATTTGGTCGT	GACAAGCTTCCCGTTCTCAG	(Wang et al., 2007)
Canine GAPDH	CTGGGGCTCACTTGAAAGG	CAAACATGGGGGCATCAG	(Fonfara et al., 2011)

Downloaded from dmd.aspetjournals.org at ASPET Journals on April 19, 2024

Figure 1

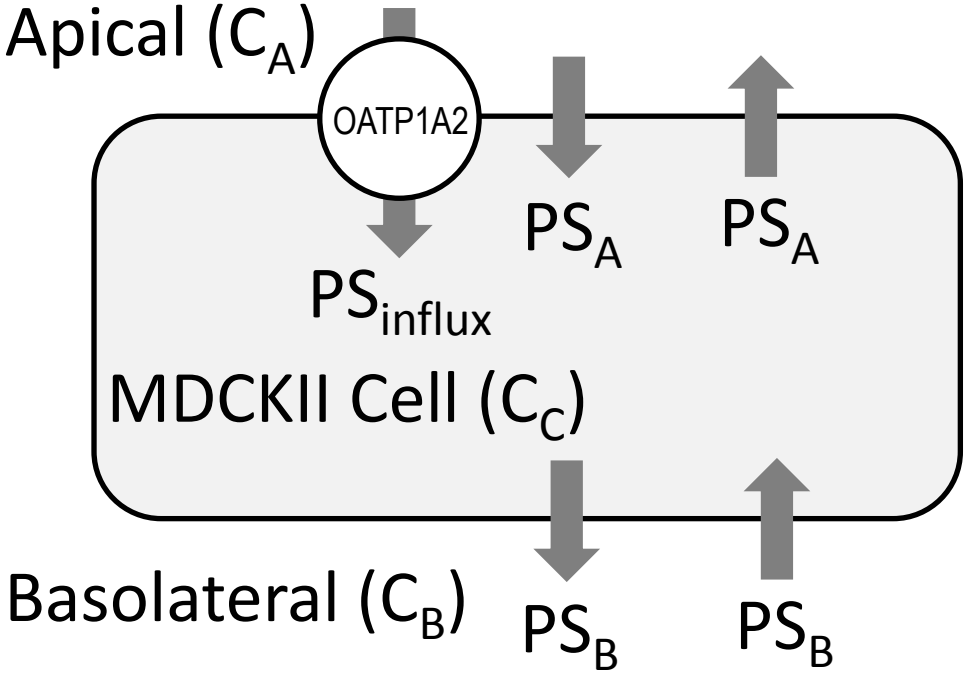

Downloaded from dmd.aspetjournals.org at ASPET Journals on April 19, 2024

Figure 2

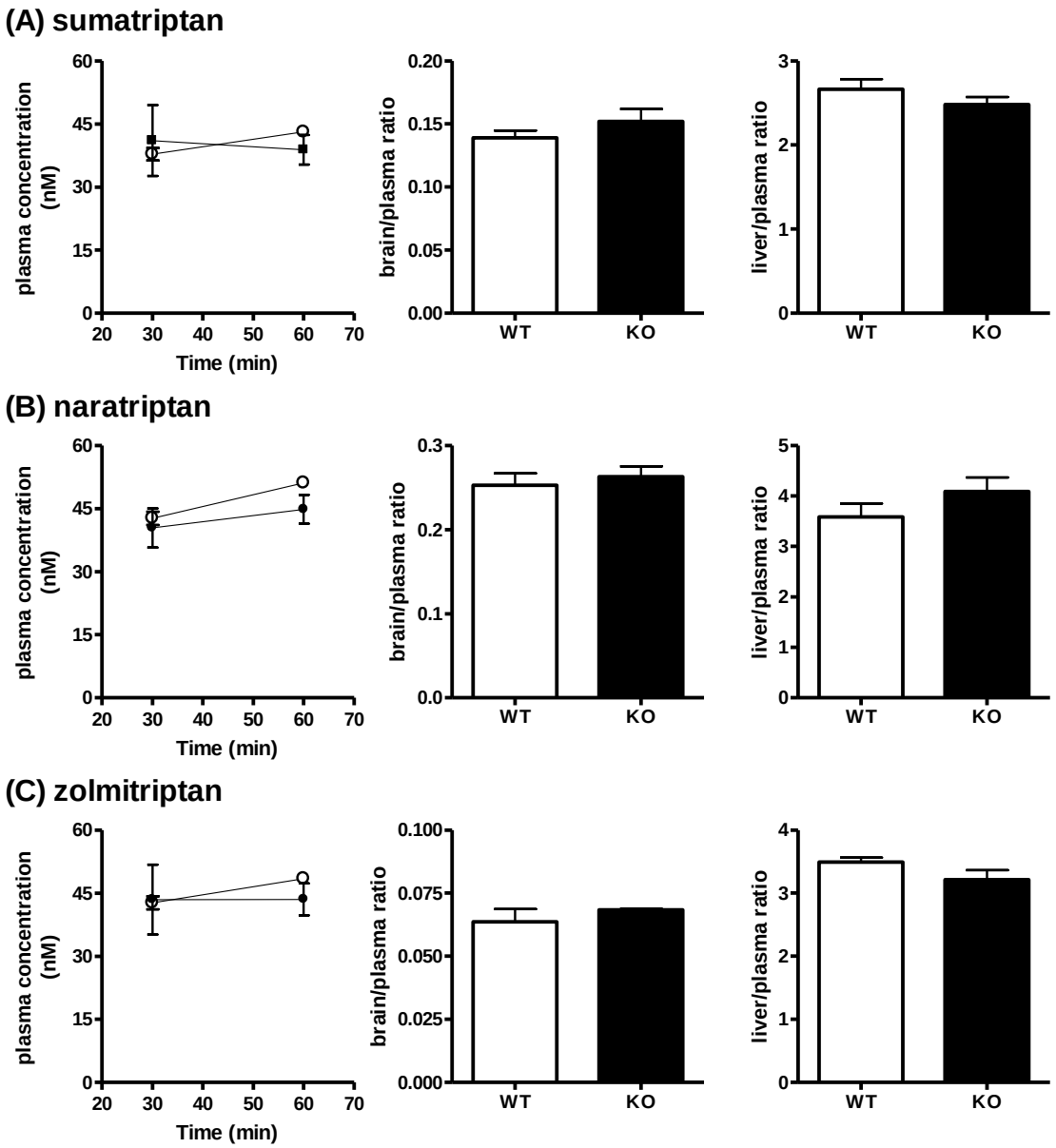

Downloaded from dmd.aspetjournals.org at ASPET Journals on April 19, 2024

Figure 3

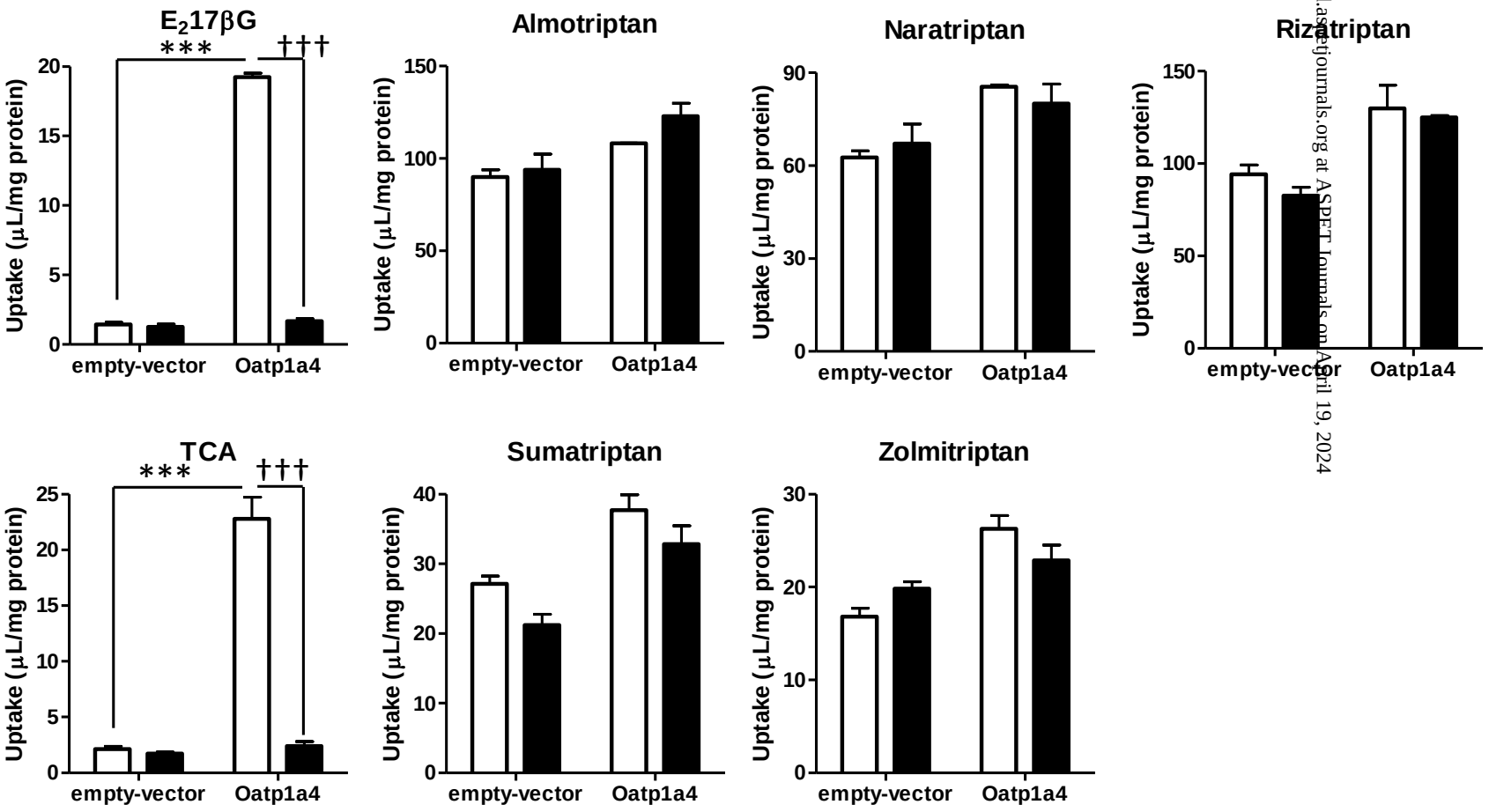

Downloaded from dmd.aspetjournals.org at ASPET Journals on April 19, 2024

Figure 4

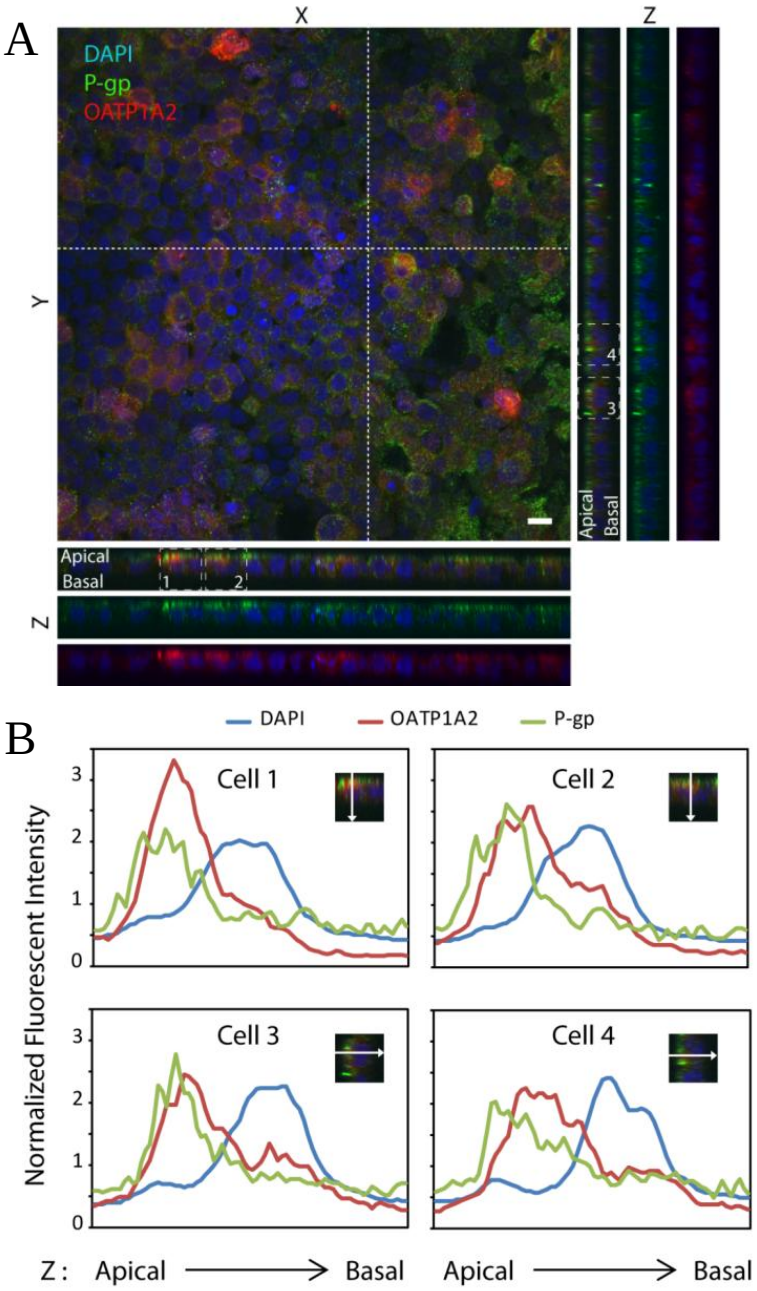

Downloaded from dmd.aspetjournals.org at ASPET Journals on April 19, 2024

Figure 5

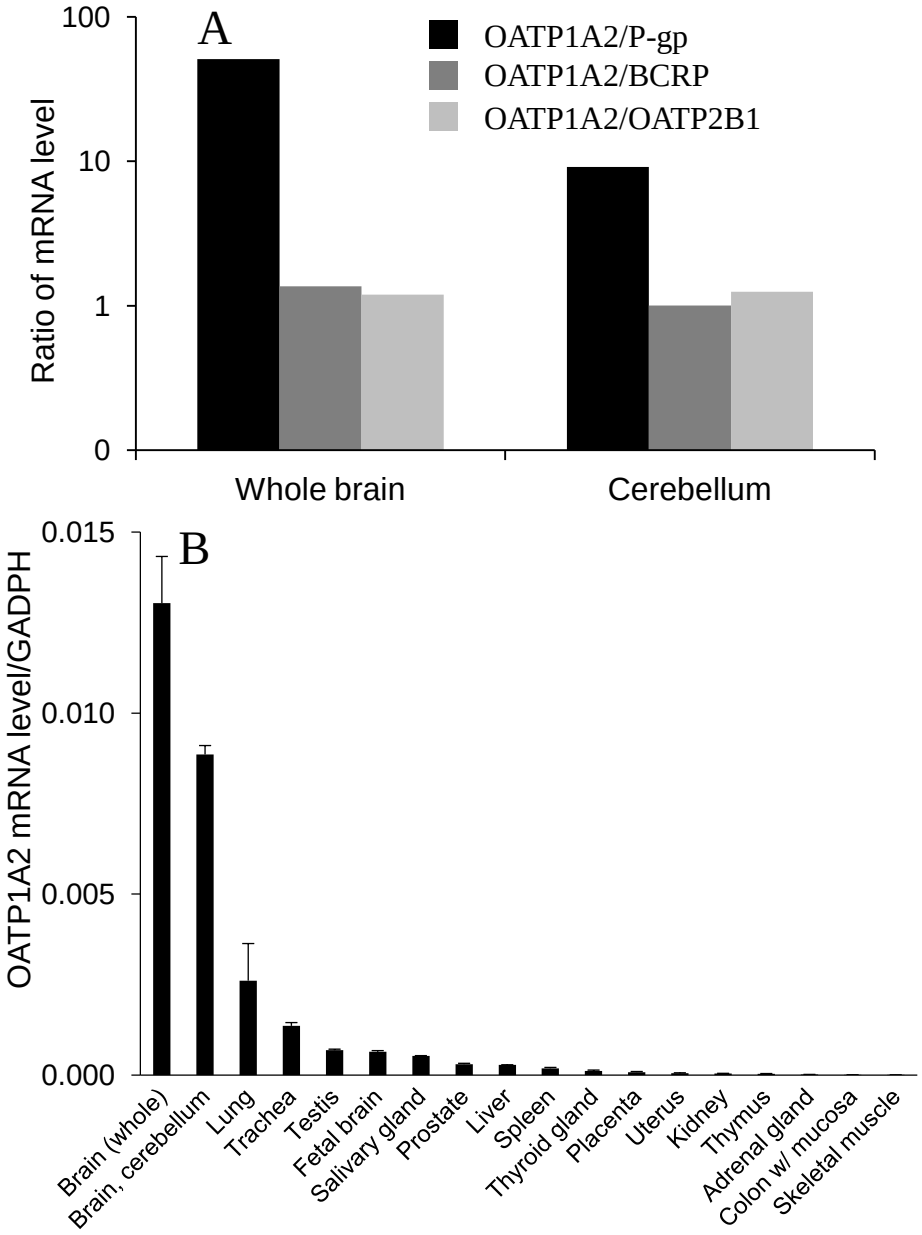

Downloaded from dmd.aspetjournals.org at ASPET Journals on April 19, 2024

Figure 6

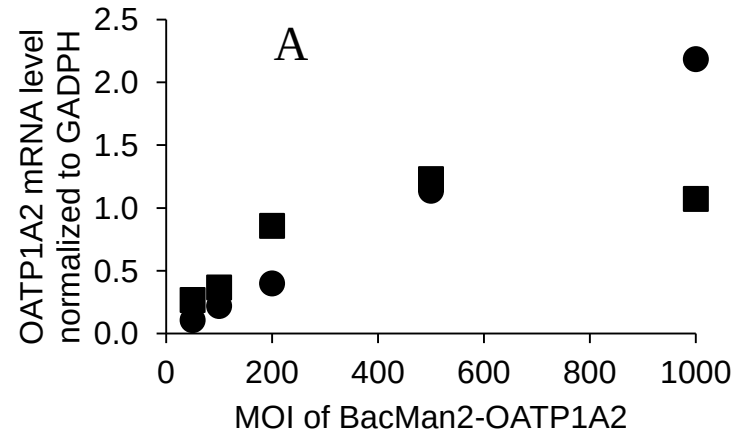

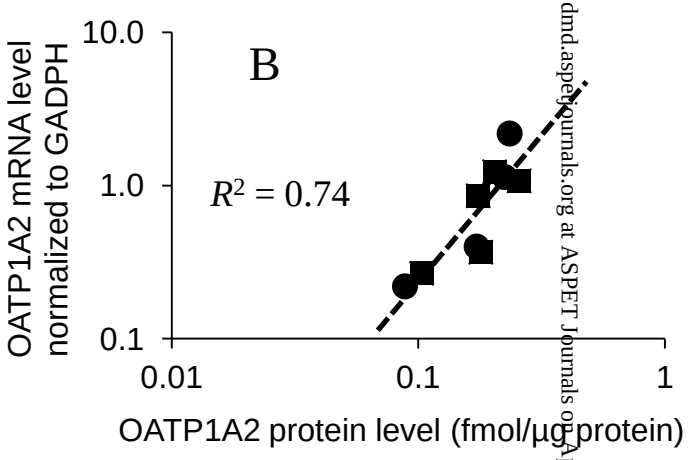

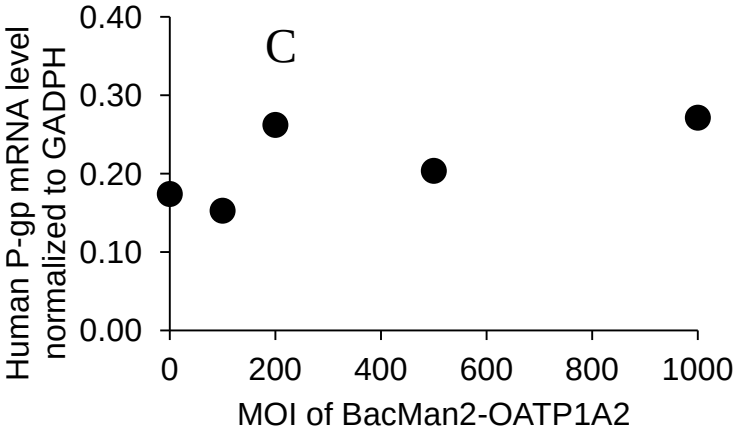

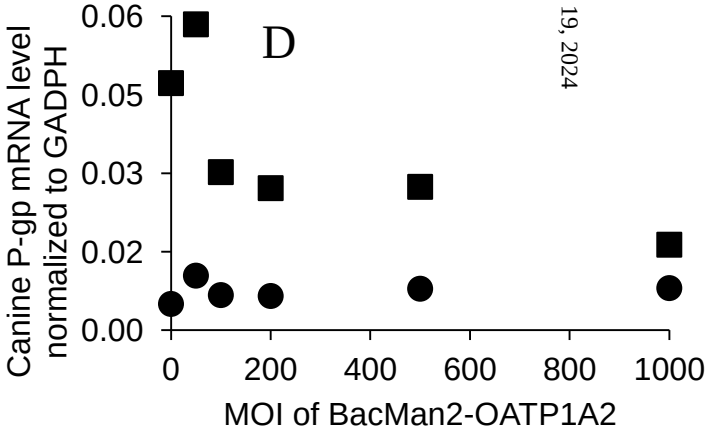

Downloaded from dmd.aspetjournals.org at ASPET Journals on April 19, 2024

Figure 7

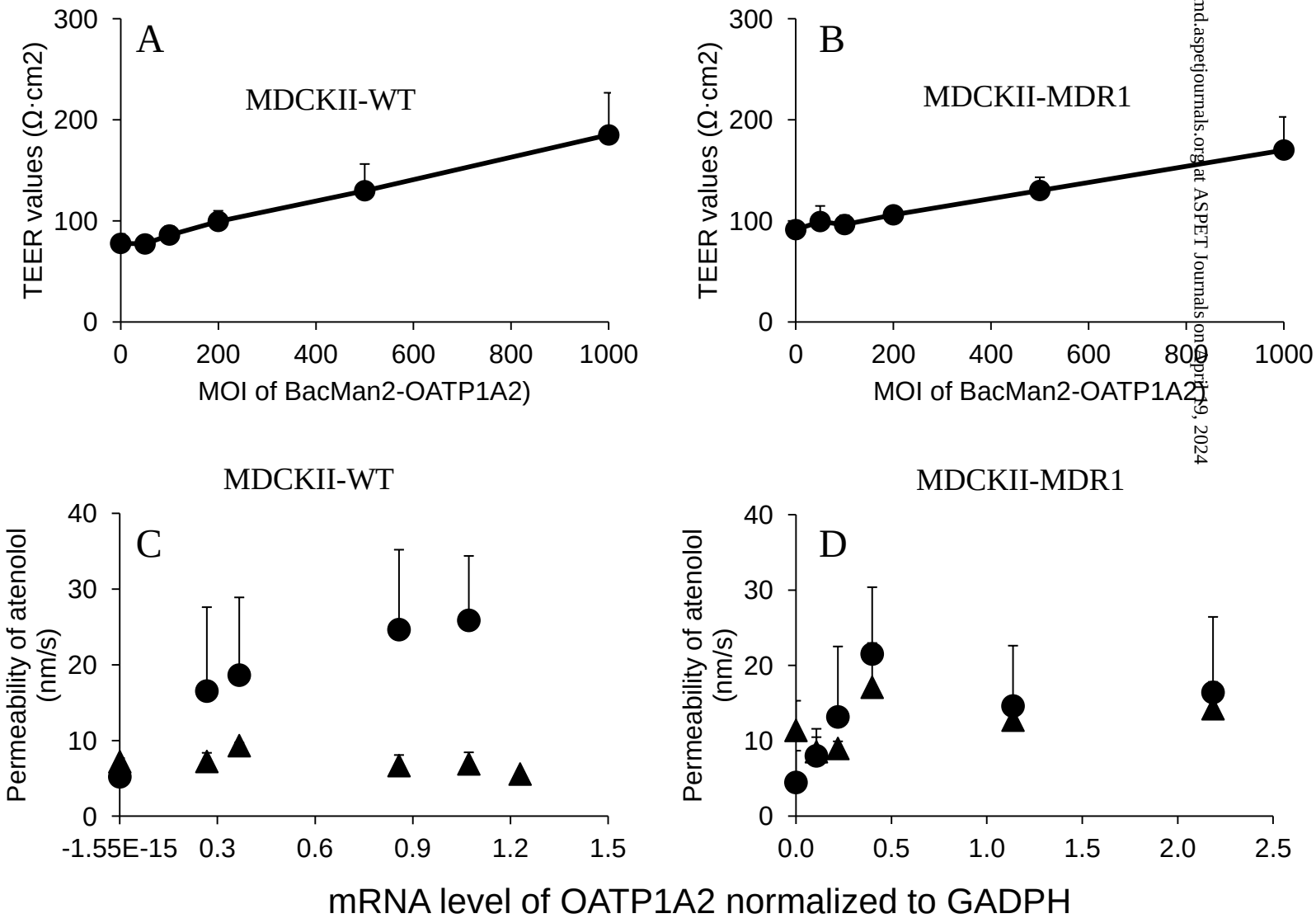

Downloaded from dmd.aspetjournals.org at ASPET Journals on April 29, 2024

Figure 8

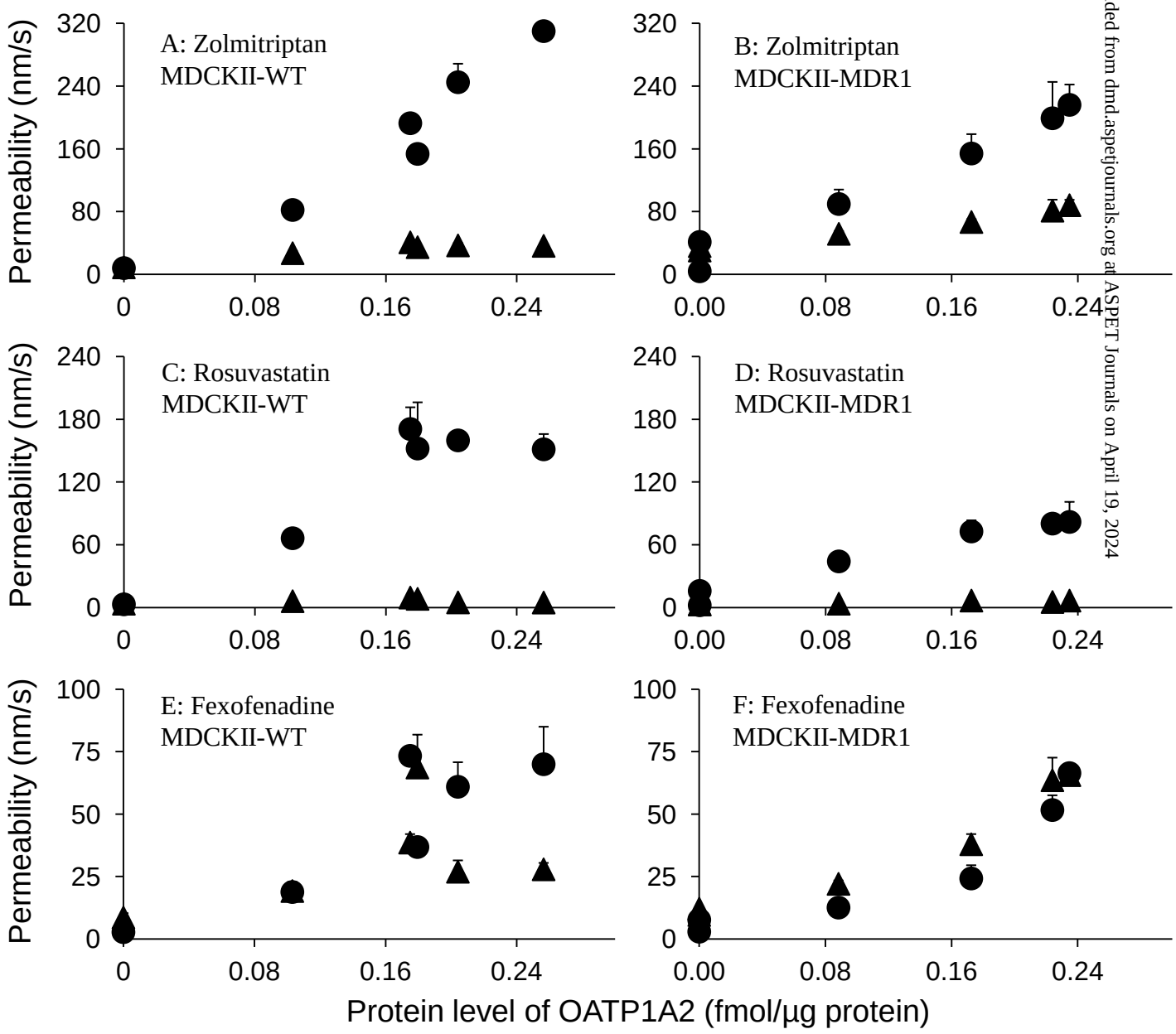

Downloaded from dmd.aspetjournals.org at ASPET Journals on April 19, 2024

Figure 9

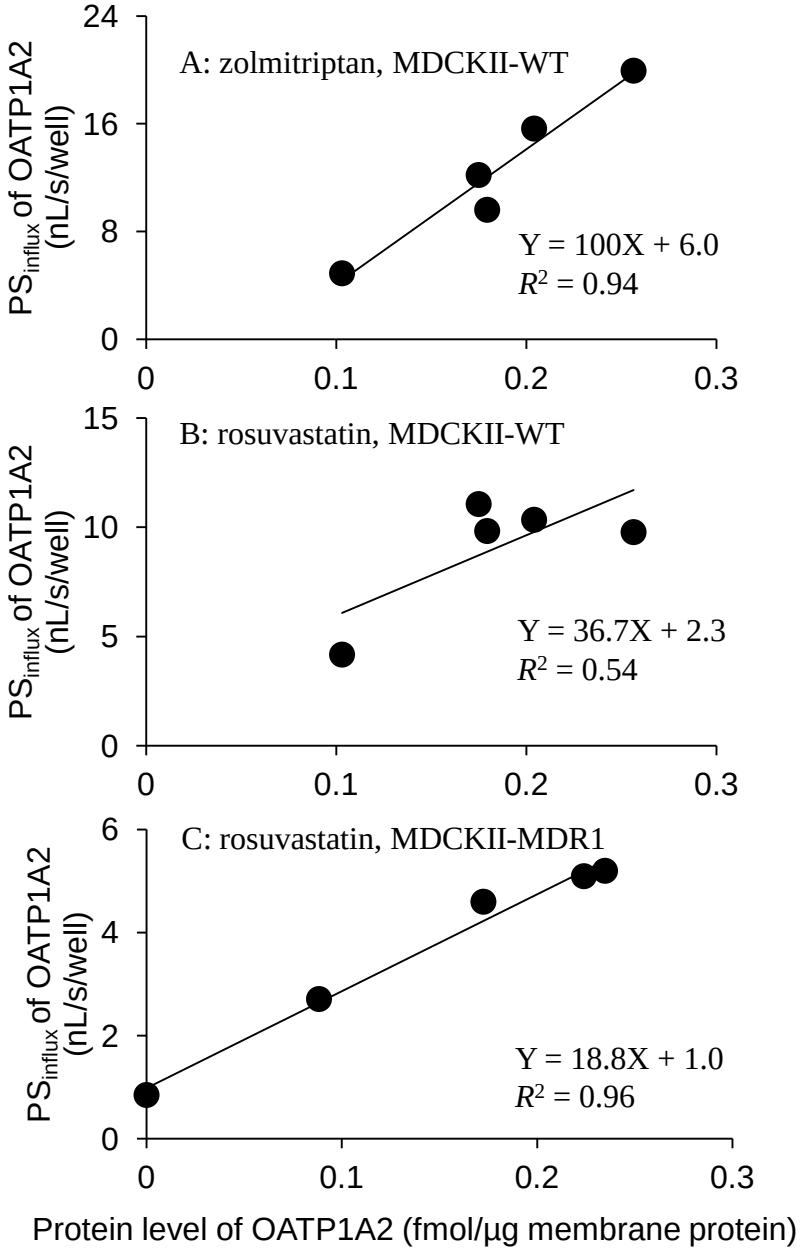

Downloaded from dmd.aspetjournals.org at ASPET Journals on April 19, 2024

Figure 10

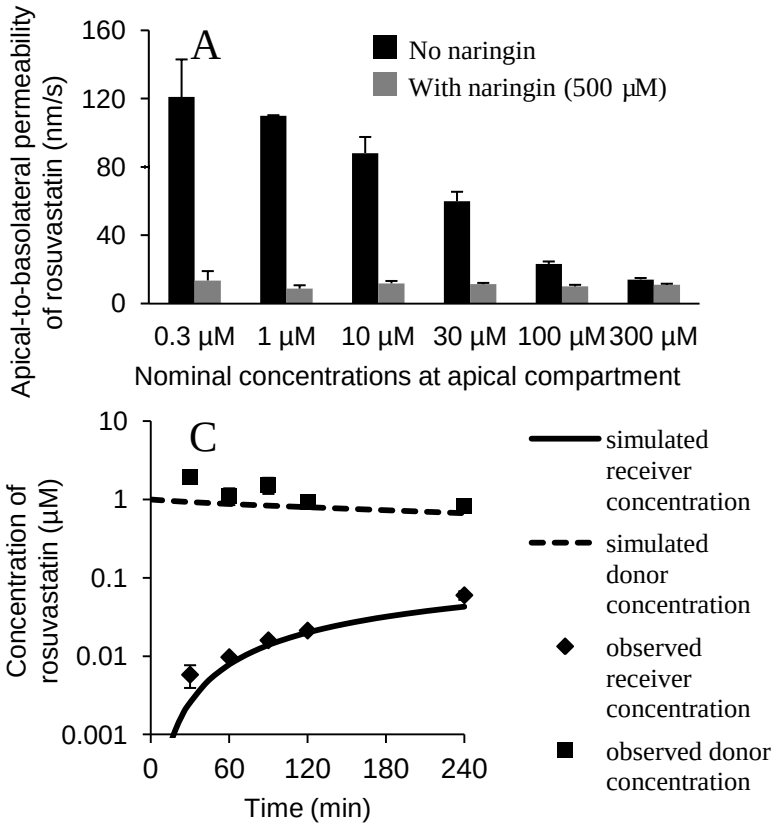

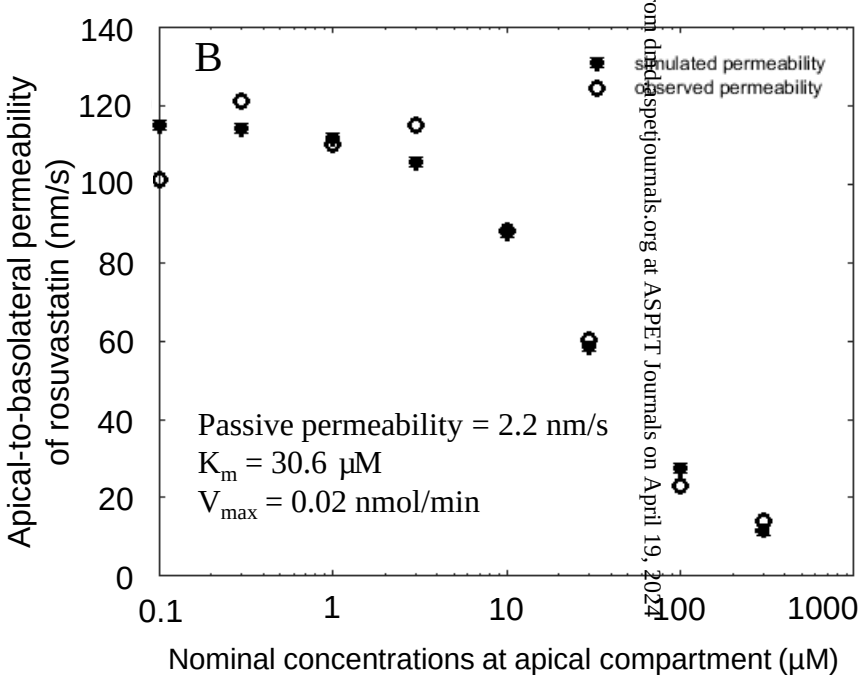

Downloaded from dmd.aspetjournals.org at ASPET Journals on April 19, 2024